



On Numerical Approximation of Diffusion Problems Governed by Variable-Exponent Nonlinear Elliptic Operators

Boris Andreianov^{1,2} · El Houssaine Quenjel³

Received: 19 April 2022 / Accepted: 5 August 2022 / Published online: 24 October 2022
© Vietnam Academy of Science and Technology (VAST) and Springer Nature Singapore Pte Ltd. 2022

Abstract

We highlight the interest and the limitations of the L^1 -based Young measure technique for studying convergence of numerical approximations for diffusion problems of the variable-exponent $p(x)$ - and $p(u)$ -laplacian kind. CVFE (Control Volume Finite Element) and DDFV (Discrete Duality Finite Volume) schemes are analyzed and tested. In the situation where the variable exponent is log-Hölder continuous, convergence is proved along the guidelines elaborated in [Andreianov et al. *Nonlinear Anal.* 72, 4649–4660, 2010 & *Nonlinear Anal.* 73, 2–24, 2010] while investigating the structural stability of weak solutions for this class of PDEs. In general, the lack of density of the smooth functions in the energy space, related to the Lavrentiev phenomenon for the associated variational problems, makes it necessary to distinguish two notions of solutions, the narrow ones (the **H**-solutions) and the broad ones (the **W**-solutions). Some situations where approximation methods “select” the one or the other of these two solution notions are described and illustrated by numerical tests.

Keywords $p(x)$ -laplacian · $p(u)$ -laplacian · Gradient finite volume approximation · Young measure · Lavrentiev phenomenon

Mathematics Subject Classification (2010) 35J60 · 65M08 · 46E35

Dedicated to Prof. Alfio Quarteroni on the occasion of his 70th anniversary.

✉ Boris Andreianov
boris.andreianov@univ-tours.fr

El Houssaine Quenjel
el-houssaine.quenjel@centralesupelec.fr

¹ Institut Denis Poisson, Université de Tours, Université d’Orléans, Parc Grandmont, Tours, 37200, France

² Peoples’ Friendship University of Russia (RUDN University), 6 Miklukho-Maklaya St., Moscow, 117198, Russian Federation

³ Chair of Biotechnology, LGPM, CentraleSupélec, CEBB, 3 rue des Rouges Terres, 51110, Pomaclé, France

1 Introduction

The token “variable-exponent problems” refers to elliptic and parabolic PDEs featuring Leray–Lions kind operators of the p -laplacian kind in which the exponent p may vary as a function of the space-time variables and even as a function of the unknown solution. In the general context of elliptic variable-exponent nonlinear diffusion problems

$$-\operatorname{div} \alpha(x, \nabla u) = f \quad \text{in } \Omega, \quad u|_{\partial\Omega} = 0, \quad (1)$$

in a bounded open domain $\Omega \subset \mathbb{R}^d$, $d \geq 1$ (we will assume Ω polygonal to make straightforward the meshing issue), as the simplest and fundamental representative problem let us consider the $p(x)$ -laplacian case:

$$\alpha(x, \nabla u) = |\nabla u|^{p(x)-2} \nabla u, \quad p : \Omega \longrightarrow (1, \infty), \quad (2)$$

(in the sequel, we will also discuss the situations where $p(\cdot)$ in (2) is itself a function of $u(\cdot)$ with a local or non-local dependence). To avoid non-essential technicalities we supplemented the PDE in (1) with the homogeneous Dirichlet boundary condition, and for the sake of simplicity the reader may think at this stage of $f \in L^\infty(\Omega)$ as a source term. Here and in the sequel, we write $p(\cdot)$ or $p(x)$ in order to stress the fact that the exponent p is a variable exponent. Following the pioneering investigations of Zhikov [53] on minimization of variable-exponent energy functionals over the adequate Sobolev-like spaces, and in relation to applications to electrorheological and thermorheological fluids [14, 51, 52] and to imaging [27], in the past twenty years there was a remarkable revival of interest to such problems witnessed in particular by the monographs [15, 30]. The goal of the present work is to discuss some aspects of numerical approximation and of numerical analysis of such variable-exponent problems.

Numerical analysis for the p -laplacian and more general Leray–Lions problems is well developed (see in particular [19, 20, 28] for the finite element analysis, [4, 9–11, 35] and the references therein for different finite volume schemes, [13] for mimetic schemes, [3, 37] for gradient schemes (encompassing many of the previous ones), [32] for a recent hybrid high-order strategy. The analysis highlights the importance of strongly consistent gradient approximation and exploits in the essential way the $L^p - L^{p'}$ duality for proving convergence of such gradient approximations via the Minty–Browder argument [25, 47, 48].

In the present contribution, we are concerned with a variety of discretization methods of the finite volume kind. The gradient reconstruction strategies elaborated for the p -laplacian remain the cornerstone for finite volume approximation of the variable-exponent problems, however, specific issues arise. There are two reasons for which the numerical analysis of the basic variable-exponent $p(x)$ -laplacian problem (1), (2) is considerably more delicate than for the case of a constant exponent p . First, a fully practical numerical method (as opposed to the theoretical Galerkin method widely used for the sake of existence proofs) makes it necessary to approximate the variable exponent map $x \mapsto p(x)$ by a sequence $(p_n(\cdot))_n$. While addressing the key issue of convergence of the (approximate) gradients ∇u_n to the gradient ∇u of the exact solution, the variable duality framework $L^{p_n(\cdot)} - L^{p'_n(\cdot)}$ requires fine adaptations of the Minty–Browder trick, such as developed by Zhikov [56–58]; such technical adaptations will be avoided in the present contribution, following the idea of [7, 8] of which the present paper is a follow-up. Second, there is an ambiguity in the choice of the underlying variable-exponent Sobolev framework, witnessed through the celebrated Zhikov counterexample ([53, 54], see also [2, 16], see Section 2). The lack of regularity of $p(\cdot)$ may lead to particular sensitivity with respect to the choice of the discretization of $p(\cdot)$,

see [41]. Moreover, it may result in the Lavrentiev phenomenon for the associated minimization problem, and in the necessity to distinguish two solution notions for the PDE at hand. The notion of **H**-solution (or narrow solution, in the sequel of this paper) appears when the solution and the test functions are sought in the closure **H**, with respect to the $p(x)$ -energy norm, of smooth compactly supported functions. The notion of **W**-solution (or broad solution, in the sequel of this paper) appears when the solution and the test functions are sought in the energy space **W** (one has $\mathbf{W} = W^{1,p(\cdot)} \cap W_0^{1,1}$ whenever the $W^{1,p(\cdot)}$ Poincaré–Friedrichs inequality holds true). According to the choice of the numerical method, convergence to the narrow or to the broad solution can be witnessed; we refer in particular to the recent work [17] in the variational setting and for finite element methods. We also refer to [24] for a *a priori* error analysis of finite element approximations of $p(x)$ -laplace problems.

The difficulties related to approximation of $p(\cdot)$ and to the choice of the functional framework are not specific to numerical approximations, they arise already in the study of the structural stability of solutions (meaning stability with respect to perturbation of data and coefficients of the problem, including the variable exponent coefficient $p(\cdot)$). Such study was conducted systematically in [7], where the framework of renormalized solutions has been chosen in order to impose the simplest possible assumptions on the perturbation of the data. As a sample result, consider a sequence $(u_n)_n$ of weak (narrow or broad, see [7] and Section 2) solutions to the Dirichlet $p(x)$ -laplacian problem with exponents $p_n(\cdot)$ and source data f_n . Assuming that $1 < p_- \leq p_n(\cdot) \leq p_+ < \infty$ and as $n \rightarrow \infty$, $p_n(\cdot) \rightarrow p(\cdot)$ in measure on Ω , that $\|f_n\|_\infty \leq \text{const}$ and $f_n \rightharpoonup f$ weakly in $L^1(\Omega)$, one finds the following results ([7], see also [59]):

- If u_n is a narrow solution of the $p_n(x)$ -laplacian problem (we mean the n -labeled problem (1), (2)) with source f_n and if for all $n \in \mathbb{N}$ one has $p_n(\cdot) \geq p(\cdot)$ a.e. in the domain Ω , then $(u_n)_n$ converges to the unique narrow solution of the $p(x)$ -laplacian problem with source f .
- If u_n is a broad solution of the $p_n(x)$ -laplacian problem with source f_n and if for all $n \in \mathbb{N}$ one has $p_n(\cdot) \leq p(\cdot)$ a.e. in the domain Ω , then $(u_n)_n$ converges to the unique broad solution of the $p(x)$ -laplacian problem with source f .
- In the situation where $p(\cdot)$ verifies the log-Hölder regularity condition of Zhikov and Fan ([39, 54, 55]; see Section 2 below for details), broad and narrow solutions of (1), (2) coincide and any sequence of (broad or narrow) weak solutions u_n of the $p_n(x)$ -laplacian problem converges, irrespective of the ordering of $p_n(\cdot)$ and $p(\cdot)$, to the unique weak solution of the limit problem.

In the present note, we combine the insight from these results and from the recent work [17] with the standard finite volume discretization framework(s) for the PDEs of p -laplacian kind. As the common guidelines of [17] and of our investigation, one can highlight the following properties:

- In the case of log-Hölder regular exponent $p(\cdot)$, convergence of several standard finite volume methods can be proved, with a wide choice of approximation strategies for $p(\cdot)$.
- Approximation of the narrow solution requires discretization of $p(\cdot)$ by $p_D = \max_D p(\cdot)$, where D denotes the generic “diamond” of the mesh on which $p(\cdot)$ is approximated; moreover, the method should be conforming in the sense that the discrete solution can be assimilated to an element of $W_0^{1,\infty}(\Omega)$.
- Approximation of the broad solution requires discretization of $p(\cdot)$ by $p_D = \min_D p(\cdot)$; moreover, the method should be able to approximate in an *ad hoc* sense the

elements of $\mathbf{W} \setminus \mathbf{H}$. While the latter property seems delicate to check theoretically (in general, it is difficult to characterize $\mathbf{W} \setminus \mathbf{H}$), it can be tested numerically, in the classical setting of the Zhikov counterexample ([2, 16, 53, 54]).

However (see Section 5) in the finite volume context, (non)conformity may have less impact on the result that the accurate choice of discretization of p .

For the sake of simplicity, we will state results for (1) only for the model $p(x)$ -laplacian case (2). However, the results we prove can be extended in a straightforward way to variable-exponent problems more general than (2), following the guidelines of [7] where a wide family of variable-exponent Leray–Lions elliptic operators for merely L^1 data was considered. Furthermore, our numerical investigation is based on the notion of a weak solution, which amounts to taking sufficient integrability assumptions on the source f so that to make unnecessary the renormalized solutions setting of [7, 21]. This restriction is due to the fact that finite volume approximation of renormalized solutions enforces the additional orthogonality restriction on the meshes and most importantly, it requires heavy technicalities, see [43, 46]. In practice, we also test our discretization techniques, on orthogonal meshes, for the case of a variable exponent thermistor problem of [56] with merely L^1 source; this test goes beyond our basic convergence analysis framework.

Furthermore, as in the sequel [8] of the work [7], we address the situations where the variable exponent depends (locally or non-locally) on the solution u itself, i.e., $p(x) = \sigma(x, u(x))$ for a sufficiently regular Carathéodory function σ . As in [8], we need the assumption of log-Hölder continuity of $\sigma(\cdot, u(\cdot))$. In practice this requires the a priori knowledge of the Hölder continuity of u and thus imposes the restriction $d < p_- = \min p(\cdot)$, where d is the space dimension. We also prospect numerically the behavior of more complex coupled problems where $p(\cdot)$ depends on $u(\cdot)$ in a non-local way (via the coupling with another differential equation driven by u), and briefly discuss the extension of the discretization techniques and of the convergence analysis to evolution problems governed by variable-exponent operators.

The outline of the paper is as follows. In Section 2 we gather the key information about variable-exponent spaces, some sample finite volume methods, and Young measures, along with the related notation. This section is by no means self-contained. Section 3 contains the theoretical and numerical results for the “robust” situations where the equality $\mathbf{W} = \mathbf{H}$ is ensured. Both $p(x)$ - and $p(u)$ - laplacian problems are addressed following closely the method of [7, 8] with the necessary adaptations to the discrete context. Section 4 is devoted to the delicate situation of “Lavrentiev gap” $\mathbf{W} \setminus \mathbf{H} \neq \emptyset$, mainly in the setting of the Zhikov counterexample.

2 Preliminaries

The goal of this section is to provide, in a sketchy way, the conceptual framework and the notation of the paper; details can be found in references.

2.1 Variable-exponent Spaces, Zhikov’s Counterexample

The solutions to problem (1), with the $p(x)$ -laplacian nonlinearity (2) are sought within the variable exponent Sobolev spaces \mathbf{H} , \mathbf{W} defined below.

Definition 1 Let $p : \Omega \rightarrow [1, +\infty)$ be a measurable function.

1. The space $L^{p(x)}(\Omega)$ consists of all measurable functions $u : \Omega \rightarrow \mathbb{R}$ such that the quantity

$$\rho_{p(x)}(f) := \int_{\Omega} |f(x)|^{p(x)} dx$$

called *the modular* is finite; on $L^{p(x)}$ one considers the Luxemburg norm

$$\|u\|_{L^{p(x)}} := \inf \{ \lambda > 0 \mid \rho_{p(x)}(u/\lambda) \leq 1 \}.$$

2. The space $W^{1,p(\cdot)}(\Omega)$ consists of all functions $u \in L^{p(\cdot)}(\Omega)$ such that the gradient ∇u of u (taken in the sense of distributions) belongs to $L^{p(\cdot)}(\Omega)$; this space is equipped with the norm

$$\|u\|_{W^{1,p(\cdot)}} := \|f\|_{L^{p(\cdot)}} + \|\nabla u\|_{(L^{p(\cdot)})^d}.$$

3. $\mathbf{H} := W_0^{1,p(\cdot)}(\Omega)$ is the closure of $C_0^\infty(\Omega)$ in the norm of $W^{1,p(\cdot)}(\Omega)$; we equip it with the norm $\|f\| := \|\nabla f\|_{(L^{p(\cdot)})^d}$.
4. \mathbf{W} is the space of all $W_0^{1,1}(\Omega)$ functions such that in addition, $\nabla u \in (L^{p(\cdot)})^d(\Omega)$, equipped with the same norm as \mathbf{H} .

When $1 < p_- \leq p(\cdot) \leq p_+ < \infty$, all the above spaces are separable reflexive Banach spaces. Many important and subtle details can be found in the monograph [30], in the papers [40] and [7] and in the references therein. We will need only a few basic properties as follows:

Proposition 1 Let $p : \Omega \rightarrow [1, \infty]$ be measurable.

1. The following form of the Hölder inequality holds true:

$$\forall f \in L^{p(\cdot)}(\Omega), g \in L^{p'(\cdot)}(\Omega), \quad \left| \int_{\Omega} f(x)g(x) dx \right| \leq 2\|f\|_{L^{p(\cdot)}} \|g\|_{L^{p'(\cdot)}},$$

where as usual, $1/p(\cdot) + 1/p'(\cdot) = 1$.

2. There holds $\rho_{p(\cdot)}(f) = 1$ if and only if $\|f\|_{L^{p(\cdot)}} = 1$.
Furthermore, if $1 \leq p_- \leq p(\cdot) \leq p_+ < \infty$, then

$$\text{whenever } \rho_{p(\cdot)}(f) \leq 1, \text{ one has } \|f\|_{L^{p(\cdot)}}^{p_+} \leq \rho_{p(\cdot)}(f) \leq \|f\|_{L^{p(\cdot)}}^{p_-};$$

$$\text{whenever } \rho_{p(\cdot)}(f) \geq 1, \text{ one has } \|f\|_{L^{p(\cdot)}}^{p_-} \leq \rho_{p(\cdot)}(f) \leq \|f\|_{L^{p(\cdot)}}^{p_+}.$$

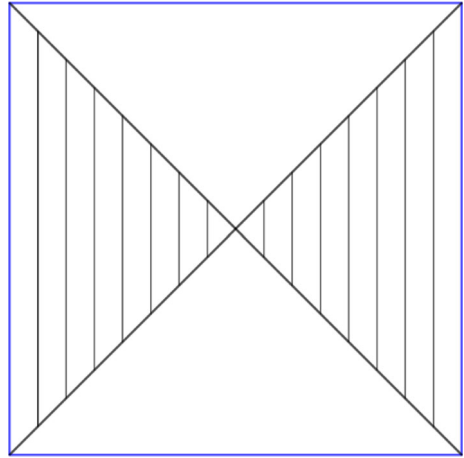
3. If, in addition, p admits a uniformly continuous on Ω representative, then the $W_0^{1,p(\cdot)}$ Poincaré–Friedrichs inequality for the norms holds:

$$\forall f \in W_0^{1,p(\cdot)}(\Omega), \quad \|f\|_{L^{p(\cdot)}} \leq \|\nabla f\|_{L^{p(\cdot)}};$$

in this case, \mathbf{W} coincides with $W_0^{1,1}(\Omega) \cap W^{1,p(\cdot)}(\Omega)$.

A difficulty in the interpretation and analysis of the variable exponent problems of the $p(x)$ -laplacian kind lies in the fact that \mathbf{H} can be a strict subspace of \mathbf{W} . Therefore, there can be at least two different ways to interpret the (1), (2) in the weak sense, according to the choice of the underlying functional space. One can avoid the difficulty by ensuring that $p(\cdot)$

Fig. 1 The setup of the (rotated, see [17]) Zhikov counterexample



satisfy the log-Hölder continuity property (3) put forward by Zhikov [54, 55] and Fan [39] and deeply exploited in [30]; the same property ensures the optimal Sobolev embedding.

Proposition 2 (see [7, Corollary 2.6]) *Assume that $p(\cdot) : \Omega \rightarrow [p_-, p_+] \subset (1, \infty)$ has a representative which can be extended into a function continuous up to the boundary $\partial\Omega$ and satisfying the log-Hölder continuity assumption:*

$$\exists L > 0, \quad \forall x, y \in \overline{\Omega}, x \neq y, \quad -(\log |x - y|) |p(x) - p(y)| \leq L. \tag{3}$$

Then the following properties hold true.

1. *The space $C_c^\infty(\Omega)$ is dense in \mathbf{W} . In particular, \mathbf{H} and \mathbf{W} can be identified.*
2. *$\mathbf{W} = \mathbf{H}$ is continuously embedded into $L^{p^*(x)}(\Omega)$, where $p^*(\cdot)$ is a measurable $(1, \infty]$ -valued optimal Sobolev embedding exponent defined as usual by the formula $p^*(x) = dp(x)/(d - p(x))$ if $p(x) < d$, $p^*(x) = \infty$ if $p(x) > d$, $p^*(x)$ is any real value if $p(x) = d$.*

The absence of (3) does not necessary lead to a discrepancy between \mathbf{W} and \mathbf{H} , indeed, other sufficient conditions for the equality $\mathbf{W} = \mathbf{H}$ exist and the counterexamples to this equality are quite scarce (see, however, [16] for recent results in this direction). Following [53] (see also [2, 16] for variants of the example; the precise formulation we take involves a rotation, like in [17]), in the square $(-1, 1)^2$ of \mathbb{R}^2 consider the piecewise constant variable exponent with a saddle-point at the origin:

$$p_0(x) = \begin{cases} 3/2 & \text{if } |x_1| < |x_2|, \\ 3 & \text{if } |x_1| > |x_2|. \end{cases} \tag{4}$$

For this choice of the domain and of the variable exponent, the above definitions lead to $\mathbf{W} \setminus \mathbf{H} \neq \emptyset$, moreover, \mathbf{H} is of co-dimension one in \mathbf{W} (see [2, 17] and references therein).

More precisely, consider the function

$$u_0(x) = \begin{cases} 1 & \text{if } |x_1| < x_2, \\ -1 & \text{if } |x_1| < -x_2, \\ \frac{x_2}{|x_1|} & \text{else,} \end{cases} \tag{5}$$

which is discontinuous at the origin (see Fig. 1). In his pioneering work [53], Zhikov showed that the singularity of u_0 cannot be approached by smooth functions in the $W^{1,p(x)}$ norm. Then, set $\tilde{u}_0(x_1, x_2) = (1 - x_1^2 - x_2^2)^+ u_0(x_1, x_2)$ to produce a function that has the same singularity as u_0 at the origin and assumes the zero Dirichlet data at the boundary of the domain $\Omega = (-1, 1)^2$. In this situation, $\tilde{u}_0 \in \mathbf{W} \setminus \mathbf{H}$ and more precisely,

$$\mathbf{W} = \mathbf{H} \oplus \text{Span}(\tilde{u}_0), \tag{6}$$

see [2] and the references therein.

2.2 CVFE and DDFV Approximations in 2D

The discrete framework we briefly describe is borrowed from the literature devoted to the standard p -laplacian. We refer to [38] for the general background on finite volume methods, to [36, 37] for a general and comparative view of the subject, to [1, 5, 26, 42] and the references therein for CVFE schemes and to [10, 34] for the DDFV schemes.

Having in mind several finite volume schemes with accurate (strongly consistent) gradient reconstruction, i.e., the so-called MPFA schemes, diamond schemes, gradient schemes etc.) let us fix a common notation which will permit to write the core of the convergence proofs disregarding the specificities of each scheme. We denote by \mathfrak{T} the control volumes of a mesh, by $u^{\mathfrak{T}}$ a generic discrete function (constant per mesh volume) on the interior volumes of the mesh. We denote by $\text{size}(\mathfrak{T})$ the maximal diameter of mesh volumes. The associated space of all discrete functions is denoted by $\mathbb{R}^{\mathfrak{T}}$. When extended by values zero at the boundary of the mesh, the discrete function is denoted by $u^{\overline{\mathfrak{T}}}$ and the associated space of all discrete functions vanishing on the mesh boundary is denoted by $\mathbb{R}_0^{\overline{\mathfrak{T}}}$. The extension to the boundary of the mesh is required to produce a discrete gradient of a discrete function.

For the sake of defining discrete vector-fields, another partition associated with the mesh \mathfrak{T} is introduced; the cells of this partition are called diamonds. We denote by $\nabla^{\mathfrak{D}} u^{\overline{\mathfrak{T}}}$ the discrete gradient, provided by the method at hand, defined on the diamond mesh denoted by \mathfrak{D} . Discrete gradients are particular instances of discrete fields, which are \mathbb{R}^2 -valued, constant per diamond functions; the space of all discrete fields is denoted by $(\mathbb{R}^2)^{\mathfrak{D}}$. Finite volume methods naturally associate to a discrete field $\mathcal{F}^{\mathfrak{D}} \in (\mathbb{R}^2)^{\mathfrak{D}}$ its discrete divergence $\text{div}^{\mathfrak{T}}[\mathcal{F}^{\mathfrak{D}}] \in \mathbb{R}^{\mathfrak{T}}$. Furthermore, two scalar products are defined: for discrete functions on the mesh \mathfrak{T} , one uses $\llbracket u^{\mathfrak{T}}, v^{\mathfrak{T}} \rrbracket$ while for discrete fields on the diamond mesh \mathfrak{D} , one uses $\llbracket \mathcal{F}^{\mathfrak{D}}, \mathcal{G}^{\mathfrak{D}} \rrbracket$. For the sake of conciseness, we will limit our attention to schemes that fulfill the following discrete duality property where we recall that $v^{\mathfrak{T}} \in \mathbb{R}^{\mathfrak{T}}$ is extended to $v^{\overline{\mathfrak{T}}} \in \mathbb{R}_0^{\overline{\mathfrak{T}}}$ by zero values at the boundary volumes:

$$\forall v^{\overline{\mathfrak{T}}} \in \mathbb{R}^{\overline{\mathfrak{T}}}, \quad \forall \mathcal{F}^{\mathfrak{D}} \in (\mathbb{R}^2)^{\mathfrak{D}}, \quad \llbracket -\text{div}^{\mathfrak{T}}[\mathcal{F}^{\mathfrak{D}}], v^{\overline{\mathfrak{T}}} \rrbracket = \llbracket \mathcal{F}^{\mathfrak{D}}, \nabla^{\mathfrak{D}} v^{\overline{\mathfrak{T}}} \rrbracket. \tag{7}$$

The precise formulas for the notation in (7) are given below for two different discretization strategies. Indeed, the two methods CVFE and DDFV that we describe in more detail below (those are the methods used for the numerical tests) both possess the property (7). Further methods successfully applied to discretization of the p -laplacian kind equations (with a fixed p) possess a variant of this property (see in particular [9, 35]); within the very general family of gradient schemes ([37]) an approximate version of the discrete duality (7) is postulated axiomatically.

Let us briefly specify the meshing, the precise meaning of the above notation, and the key definitions of the operators $\nabla^{\mathcal{D}}$, $\text{div}^{\mathcal{T}}$ for the CVFE and the DDFV schemes. Note that the general approach to convergence analysis followed in this paper applies to other schemes in 2D or in 3D that enjoy the Discrete Duality property, such as the NDD (Nodal Discrete Duality) scheme recently developed by the authors in [12].

2.2.1 CVFE Method

Given a conforming triangular primal mesh \mathcal{D} in the sense of the finite elements, the principle of the CVFE method is to consider scalar unknowns $u^{\mathcal{T}}$ on the dual mesh $\overline{\mathcal{T}}$ (built on \mathcal{D}) while the gradient operator $\nabla^{\mathcal{D}}$ is defined on the triangles of \mathcal{D} (see, e.g., [1, 5, 26, 42]). A generic triangle is denoted by D .

The dual mesh $\overline{\mathcal{T}}$ is centered on the vertices of the triangular mesh \mathcal{D} . For each vertex \mathbf{v} , the associated unique control volume $K_{\mathbf{v}}$ or simply K is obtained by connecting the barycenter of the elements, having in common \mathbf{v} , to the centers of the edges sharing the same vertex. We denote by \mathcal{E}_K the set containing the edges of K . The scalar product $\llbracket \cdot, \cdot \rrbracket$ can be expressed as

$$\llbracket u^{\mathcal{T}}, v^{\mathcal{T}} \rrbracket = \sum_{K \in \overline{\mathcal{T}}} |K| u_K v_K,$$

where $|K|$ stands for the measure of K . The discrete gradient is defined as in the finite element literature (see, e.g. [50]), meaning that

$$\nabla^{\mathcal{D}} u^{\mathcal{T}} = \sum_{K \in \overline{\mathcal{T}}} u_K \nabla \varphi_K,$$

where $(\varphi_K)_{K \in \overline{\mathcal{T}}}$ is the basis of \mathbb{P}_1 shape functions on the triangular mesh $\overline{\mathcal{T}}$. The function $\nabla^{\mathcal{D}} u^{\mathcal{T}}$ is constant per element of \mathcal{D} , therefore one can consider $\nabla^{\mathcal{D}} u^{\mathcal{T}}$ as belonging to the space $(\mathbb{R}^{\mathcal{D}})^2$ of discrete fields on Ω . The scalar product $\llbracket \cdot, \cdot \rrbracket$ on $(\mathbb{R}^{\mathcal{D}})^2$ is defined for $\mathcal{F}^{\mathcal{D}} = (\mathcal{F}_D)_{D \in \mathcal{D}}$, $\mathcal{G}^{\mathcal{D}} = (\mathcal{G}_D)_{D \in \mathcal{D}}$ merely by

$$\llbracket \mathcal{F}^{\mathcal{D}}, \mathcal{G}^{\mathcal{D}} \rrbracket = \sum_{D \in \mathcal{D}} |D| \mathcal{F}_D \cdot \mathcal{G}_D. \tag{8}$$

Let $\mathcal{F}^{\mathcal{D}}$ belong to $(\mathbb{R}^2)^{\mathcal{D}}$, the discrete divergence of $\mathcal{F}^{\mathcal{D}}$ within K is defined by

$$\text{div}^{\mathcal{T}}[\mathcal{F}^{\mathcal{D}}]_{|K} = \frac{1}{|K|} \sum_{\sigma \in \mathcal{E}_K} |\sigma| \mathcal{F}^{\mathcal{D}} \cdot \mathbf{n}_{\sigma},$$

where $|\sigma|$ is the length of the interface σ and \mathbf{n}_{σ} accounts for the outward unit normal to σ .

The discrete duality (7) for this CFVE method on triangles holds true, moreover, note that it is possible to extend the method to primal mesh consisting of arbitrary polygons while keeping the discrete duality ([5]), though issues with scheme coercivity may arise.

Finally, note that source terms f in CVFE setting are discretized by $f^{\mathcal{T}} = (f_K)_{K \in \overline{\mathcal{T}}}$ with either the mean-value choice (the L^1 integrability of f is enough) or the center-value choice (whenever f is continuous on K):

$$f_K = \frac{1}{|K|} \int_K f(x) dx \text{ (mean value)} \quad \text{or} \quad f_K = f(x_K) \text{ (center value)}. \tag{9}$$

The discretization of the source term is strongly consistent in the sense that if $f \in L^p(\Omega)$, $p < \infty$, and $(u^{\mathcal{T}})_{\overline{\mathcal{T}}}$ is a sequence of discrete functions weakly convergent in $L^{p'}(\Omega)$ to a

limit u as the discretization step size (\mathfrak{T}) of the mesh \mathfrak{T} goes to zero, then

$$\left[f^{\mathfrak{T}}, u^{\mathfrak{T}} \right] \rightarrow \int_{\Omega} f(x)u(x) dx \quad \text{as } \text{size}(\mathfrak{T}) \rightarrow 0; \tag{10}$$

moreover, the gradient discretization is strongly consistent in the sense that if $\phi \in C_c^\infty(\Omega)$ is discretized by $\phi^{\mathfrak{T}} = (\phi(x_K))_{K \in \mathfrak{T}}$, there holds

$$\nabla^{\mathfrak{D}} \phi^{\mathfrak{T}} \rightarrow \nabla \phi \quad \text{a.e. on } \Omega \text{ and in } (L^p(\Omega))^2, \text{ for all } p < \infty \tag{11}$$

as $\text{size}(\mathfrak{T}) \rightarrow 0$ (see, e.g., [50]); moreover, the per diamond gradient discretization is first-order accurate (it is exact on functions affine in a neighborhood of a given diamond).

Finally, we point out that the discrete duality (7) ensures that for a family of meshes with $\text{size}(\mathfrak{T})$ going to zero, weak L^1 limits of discrete functions and the associated discrete gradients are linked by the continuous gradient operator:

$$\left. \begin{aligned} u^{\mathfrak{T}} \rightharpoonup u \text{ in } L^1(\Omega) \text{ weakly} \\ \nabla^{\mathfrak{D}} u^{\mathfrak{T}} \rightharpoonup \mathcal{G} \text{ in } (L^1(\Omega))^2 \text{ weakly} \end{aligned} \right\} \implies u \in W_0^{1,1}(\Omega) \text{ and } \mathcal{G} = \nabla u. \tag{12}$$

The CVFE method can be seen as a lumped Finite Element method, indeed, only the discretization of the source term, based on the mass lumping idea, differs from the Finite Element framework. In particular, while in CVFE context one associates to a discrete function $u^{\mathfrak{T}}$ the piecewise constant on Ω function $u^{\mathfrak{T}}(x) = \sum_{K \in \mathfrak{T}} u_K \mathbb{1}_K$, one can also exploit the continuous, affine per diamond reconstruction.

2.2.2 DDFV Method

The particularity of the DDFV discretization is the construction of the whole discrete gradient on the diamond mesh \mathfrak{D} requiring two different partitions of Ω , namely the primal mesh \mathfrak{M} and dual mesh $\overline{\mathfrak{M}^*}$ (if one considers only the inner volumes \mathfrak{M}^* of the dual mesh, it does not cover the whole of Ω).

The primal mesh \mathfrak{M} is a set of control volumes K covering $\overline{\Omega}$. The volumes of the dual mesh are defined on \mathfrak{M} around the vertices. Each dual cell of $\overline{\mathfrak{M}^*}$ corresponds to a vertex of \mathfrak{M} , the boundary cells corresponding to the vertices of the primal mesh that lie on $\partial\Omega$. These dual cells are obtained by connecting the centers of primal cells of \mathfrak{M} sharing the vertex in question. The diamond mesh is made from quadrilaterals (resp. triangles) built on the internal (resp. external) edges of \mathfrak{M} .

Then, we denote $\overline{\mathfrak{T}} = \overline{\mathfrak{M}} \cup \overline{\mathfrak{M}^*}$ (the boundary volumes of the primal mesh which are degenerate flat portions of the boundary $\partial\Omega$). The unknowns are attached only to the inner volumes of each mesh, so that $u^{\mathfrak{T}} = (u^{\mathfrak{M}}, u^{\mathfrak{M}^*})$. For the sake of the gradient discretization and having in mind the homogeneous Dirichlet condition (extension to inhomogeneous Dirichlet condition is described in [10]), the values of $u^{\overline{\mathfrak{T}}}$ in the primal and dual boundary volumes are set to zero. In the DDFV setting, the inner product $\llbracket \cdot, \cdot \rrbracket$ involves primal and dual unknowns. It writes

$$\llbracket u^{\overline{\mathfrak{T}}}, v^{\overline{\mathfrak{T}}} \rrbracket = \frac{1}{2} \sum_{K \in \mathfrak{M}} |K| u_K v_K + \frac{1}{2} \sum_{K^* \in \mathfrak{M}^*} |K^*| u_{K^*} v_{K^*}.$$

Consider a diamond cell D with diagonals $(\sigma, \sigma^*) \in \mathcal{E}_K \times \mathcal{E}_{K^*}$. In fact, the interface $\sigma = K|L$ is shared by two primal volumes K and L . This notation also covers boundary edges seen as degenerate volumes by convention. The dual edge $\sigma = K^*|L^*$ is shared by two dual

cells K^*, L^* corresponding to the end point of σ . The discrete gradient on the diamond D is defined in the 2D basis $(\mathbf{n}_{KL}, \mathbf{n}_{K^*L^*})$ by the formula

$$\nabla^{\mathcal{D}} u_{|D}^{\overline{\mathcal{F}}} = \frac{1}{2|D|} (|\sigma|(u_L - u_K)\mathbf{n}_{KL} + |\sigma^*|(u_{L^*} - u_{K^*})\mathbf{n}_{K^*L^*}),$$

where \mathbf{n}_{KL} (resp. $\mathbf{n}_{K^*L^*}$) denotes the unit normal to σ (resp. σ^*) pointing from K to L (resp. from K^* to L^*), and $|\sigma|, |\sigma^*|$ stand for the length of the respective edges. The function $\nabla^{\mathcal{D}} u_{|D}^{\overline{\mathcal{F}}}$, constant per diamond, can be seen as an element of the space $(\mathbb{R}^{\mathcal{D}})^2$ of discrete fields. As in the CVFE context, the scalar product on $(\mathbb{R}^{\mathcal{D}})^2$ is defined by (8). Also the divergence operator is defined in the traditional way of finite volume schemes, but separately on the primal and dual meshes as follows:

$$\operatorname{div}^{\mathcal{F}}[\mathcal{F}^{\mathcal{D}}]_{|K} = \frac{1}{|K|} \sum_{\sigma \in \mathcal{E}_K} |\sigma| \mathcal{F}^{\mathcal{D}} \cdot \mathbf{n}_{\sigma}, \quad \operatorname{div}^{\mathcal{F}}[\mathcal{F}^{\mathcal{D}}]_{|K^*} = \frac{1}{|K^*|} \sum_{\sigma^* \in \mathcal{E}_{K^*}} |\sigma^*| \mathcal{F}^{\mathcal{D}} \cdot \mathbf{n}_{\sigma^*}.$$

The discrete duality (the formula (7)), which gave its name to the DDFV method, holds true ([10]). Note that the DDFV method allows for two different 3D extensions; in the present contribution we limit our attention to 2D tests, but the analytical proof works as well for the 3D DDFV schemes of [29] and [4].

Finally, we stress that in the DDFV method, the identification of a discrete function $u^{\mathcal{F}} = (u^{\mathfrak{M}}, u^{\mathfrak{M}^*})$ to a piecewise constant function on Ω is done through the formula

$$u^{\mathcal{F}}(x) = \frac{1}{2} \sum_{K \in \mathfrak{M}} u_K \mathbb{1}_K + \frac{1}{2} \sum_{K^* \in \mathfrak{M}^*} u_{K^*} \mathbb{1}_{K^*}. \tag{13}$$

Source terms are discretized analogously (9) on the primal and on the dual mesh. Having in mind the convention (13), the properties (10), (11) (along with the order one consistency of the gradient reconstruction) and (12) hold true (see, e.g., [10]). Note that in presence of u -dependent nonlinear terms, such as for the $p(u)$ -laplacian considered in Section 3.2 below, a penalization of $u^{\mathfrak{M}} - u^{\mathfrak{M}^*}$ is needed for the convergence analysis (see [4, 6] for details).

2.3 Young Measures and Nonlinear weak-* Convergence

In the following theorem, limiting our attention to the case of a bounded domain Ω , we state the well-known results taken from Ball [18], Pedregal [49] and (for the version stated below) Hungerbühler [44] on the generation of Young measures for equi-integrable sequences of $L^1(\Omega)$ functions, and on the reduction of Young measures. These results are at the core of our convergence analysis.

Here and in the sequel, the notation δ_0 will be used for the standard Dirac measure concentrated at the origin of \mathbb{R}^d , while $\delta_c(\cdot) := \delta_0(\cdot - c)$. We underline the use of the convergence in measure on Ω , for a sharp statement of the reduction result.

Theorem 3 *Let $\Omega \subset \mathbb{R}^N$, $N \in \mathbb{N}$, be a bounded domain.*

- (i) *Let $(v_n)_n$ be a sequence of \mathbb{R}^d -valued functions on Ω , $d \in \mathbb{N}$, such that $(v_n)_n$ is equi-integrable on Ω . Then there exists a subsequence $(n_k)_k$ and a parametrized family $(\nu_x)_{x \in \Omega}$ of probability measures on \mathbb{R}^d , weakly measurable in x with respect to the Lebesgue measure on Ω , such that for all continuous function $F : \mathbb{R}^d \mapsto \mathbb{R}^t$, $t \in \mathbb{N}$, we have*

$$\lim_{k \rightarrow +\infty} \int_{\Omega} F(v_{n_k}(x)) dx = \int_{\Omega} \int_{\mathbb{R}^d} F(\lambda) d\nu_x(\lambda) dx \tag{14}$$

whenever the sequence $(F(v_n(\cdot)))_n$ is equi-integrable on Ω . In particular,

$$v(x) := \int_{\mathbb{R}^d} \lambda \, d\nu_x(\lambda)$$

is the weak limit of the sequence $(v_{n_k})_k$ in $L^1(\Omega)$, as $k \rightarrow +\infty$. The family $(\nu_x)_x$ is called the Young measure generated by the subsequence $(v_{n_k})_k$.

- (ii) If $(\nu_x)_x$ is the Young measure generated by a sequence $(v_n)_n$, then

$$\nu_x = \delta_{v(x)} \text{ for a.e. } x \in \Omega \iff v_n \rightarrow v \text{ in measure as } n \rightarrow +\infty.$$

- (iii) If $(u_n)_n$ generates a Dirac Young measure $(\delta_{u(x)})_x$ on \mathbb{R}^{d_1} , and $(v_n)_n$ generates a Young measure $(\nu_x)_x$ on \mathbb{R}^{d_2} , then the sequence $((u_n, v_n))_n$ generates the Young measure $(\delta_{u(x)} \otimes \nu_x)_x$ on $\mathbb{R}^{d_1+d_2}$.

3 The Regular Exponent Case

In this section, we assume that $p(\cdot)$ fulfills (3) and consequently, Proposition 2 holds true. In this case, the notion of solution for problem (1), (2) is fairly standard.

Definition 2 Assume $p(\cdot)$ fulfills (3) and $f \in L^{(p^*)'}(\Omega)$. A weak solution of the homogeneous Dirichlet $p(x)$ -laplacian problem (1), (2) is a function $u \in \mathbf{W} = \mathbf{H}$ that fulfills $-\operatorname{div} a(x, \nabla u) = f$ in the sense of distributions. Equivalently, this means

$$u \in \mathbf{W} = \mathbf{H} \text{ s.t. } \forall \phi \in \mathbf{W} = \mathbf{H}, \int_{\Omega} a(x, \nabla u(x)) \cdot \nabla \phi(x) \, dx = \int_{\Omega} f(x)\phi(x) \, dx. \tag{15}$$

We will strengthen the assumption of integrability on f to $f \in L^{(p-)'}$ for the sake of providing the essential arguments assessing convergence of CVFE and DDFV approximations of problem (1), (2).

3.1 Convergence of CVFE and DDFV Finite Volume Schemes for the $p(x)$ -Laplacian

The central result of the paper is the following theorem, where we focus on the simple setting to avoid the non-essential technicalities and put clearly the core arguments.

Theorem 4 On a bounded polygonal open domain Ω of \mathbb{R}^2 , consider the nonlinear elliptic Dirichlet problem (1) with the $p(x)$ -laplacian nonlinearity (2) for a variable exponent $p(\cdot)$ verifying the log-Hölder regularity assumption (3).

Consider a family $(\mathfrak{T}_n)_n$ of CVFE or DDFV meshes of Ω with the associated diamond meshes $(\mathfrak{D}_n)_n$ of size going to zero as $n \rightarrow \infty$. Assume that the discrete Poincaré–Friedrichs inequality in L^q , $q \in [1, \infty)$, with a uniform in n constant¹, holds for the family of meshes $(\mathfrak{T}_n)_n$. Regarding the discretization $p^{\mathfrak{D}_n} = (p_D)_{D \in \mathfrak{D}_n} \in \mathbb{R}^{\mathfrak{D}_n}$ of the variable exponent $p(\cdot)$ on the diamond mesh, we merely assume that for each $D \in \mathfrak{D}_n$,

¹Proofs of discrete Poincaré inequality in the Finite Volume literature often require an assumption of regularity of the family of meshes, cf. [38]; note however that in many situations including DDFV and CVFE with homogeneous Dirichlet boundary condition, the technique of [11, Lemma 2.6(i)] permits to drop the regularity assumptions of [38], cf. the discussion in [10, Sect. III.B].

$p_D \in [p_-, p_+]$ is chosen so that

$$\min_D p(\cdot) \leq p_D \leq \max_D p(\cdot). \tag{16}$$

Assume $f \in L^{(p_-)'}(\Omega)$ and consider the mean-value discretization $f^{\mathfrak{T}_n} \in \mathbb{R}^{\mathfrak{T}_n}$ as in (9) (if f is piecewise continuous, center-value discretization can be considered instead). Consider the family of discrete problems written in the variational form:

$$\begin{aligned} \text{find } u^{\mathfrak{T}_n} \in \mathbb{R}^{\mathfrak{T}_n} \text{ such that } \forall \phi^{\mathfrak{T}_n} \in \mathbb{R}^{\mathfrak{T}_n} \\ \left\{ \left\{ \alpha^{\mathfrak{D}_n}(\cdot, \nabla^{\mathfrak{D}_n} u^{\mathfrak{T}_n}), \nabla^{\mathfrak{D}_n} \phi^{\mathfrak{T}_n} \right\} \right\} = \left[\left[f^{\mathfrak{T}_n}, \phi^{\mathfrak{T}_n} \right] \right], \end{aligned} \tag{17}$$

where on each diamond $D \in \mathfrak{D}$, the approximation of $\alpha(\cdot, \xi) = |\xi|^{p(\cdot)-2}\xi$ is chosen to be

$$\alpha^{\mathfrak{D}}(\cdot, \xi) = |\xi|^{p_D-2}\xi.$$

For all $n \in \mathbb{N}$, the scheme admits a unique solution $u^{\mathfrak{T}_n}$ that we assimilate to a piecewise constant function on Ω . As $n \rightarrow \infty$, there holds

$$u^{\mathfrak{T}_n} \rightarrow u \quad \text{and} \quad \nabla^{\mathfrak{D}_n} u^{\mathfrak{T}_n} \rightarrow \nabla u \quad \text{a.e. on } \Omega, \tag{18}$$

moreover the associated energies converge:

$$\left| \nabla^{\mathfrak{D}_n} u^{\mathfrak{T}_n} \right|^{p^{\mathfrak{D}_n}} \rightarrow |\nabla u|^{p(\cdot)} \quad \text{in } L^1(\Omega), \tag{19}$$

where u is the unique weak solution in the sense of Definition 2 of (1), (2).

It is not difficult to upgrade the a.e. convergence of the discrete solutions and their gradients to convergence in some fixed or variable exponent Lebesgue spaces, using (18), (19), De La Vallée Poussin equi-integrability property with the Vitali theorem, and the embeddings stated in Proposition 2. However, unless we make the assumption $p_D = \max_D p(\cdot)$, one cannot reach the $L^{p(\cdot)}(\Omega)$ convergence of the gradients. In this direction, the sharpest convergence result is (19) hereabove; it is also of interest for readers interested in the approximation of the variational problem underlying (1), (2).

Furthermore, scheme (17) can be rewritten into the standard per-volume form by taking $v^{\mathfrak{T}_n}$ in (17) with one entry equal to 1 and all the others equal to zero.

In addition to the key properties of the CVFE and DDFV schemes pointed out in Section 2.2, we will use further standard properties of the CVFE and DDFV schemes such as the inequality

$$\left[\left[f^{\mathfrak{T}}, u^{\mathfrak{T}} \right] \right] \leq \text{const} \|f\|_{L^{q'}(\Omega)} \|\nabla^{\mathfrak{D}} u^{\mathfrak{T}}\|_{L^q(\Omega)} \tag{20}$$

valid for any constant value $q \in (1, \infty)$ due in particular to the discrete Poincaré–Friedrichs inequality (see, e.g., [23] and the references therein). Note that we will not develop $p(x)$ -versions of this inequality, taking the simplifying assumption $f \in L^{(p_-)'}(\Omega)$.

Proof The proof is structured into several steps. For the sake of legibility we will drop the subscript n and write $\text{size}(\mathfrak{T}) \rightarrow 0$ in the place of $n \rightarrow \infty$.

Step 1. Assuming that $u^{\mathfrak{T}}$ is a solution to (17), we take $\phi^{\mathfrak{T}} = u^{\mathfrak{T}}$ as the test function and find

$$\rho_{p^{\mathfrak{D}}(\cdot)}(\nabla^{\mathfrak{D}} u^{\mathfrak{T}}) = \int_{\Omega} \left| \nabla^{\mathfrak{D}} u^{\mathfrak{T}}(x) \right|^{p^{\mathfrak{D}}(x)} dx = \left[\left[f^{\mathfrak{T}}, u^{\mathfrak{T}} \right] \right], \tag{21}$$

where we can apply (20) with the constant exponent $q = p_-$ to upper bound the right-hand side (under the regularity assumptions on the family of meshes that guarantee a uniform constant in the discrete L^q -Poincaré–Friedrichs inequality). This entails the uniform in $\text{size}(\mathfrak{T})$ bound

$$\rho_{p^\mathfrak{D}(\cdot)}(\nabla^\mathfrak{D} u^\mathfrak{T}) \leq \text{const} \quad \text{uniformly in } \text{size}(\mathfrak{T}). \tag{22}$$

Indeed, having in mind (16), for all $x \in \Omega$ there holds

$$\left| \nabla^\mathfrak{D} u^\mathfrak{T}(x) \right|^{p_-} \leq 1 + \left| \nabla^\mathfrak{D} u^\mathfrak{T}(x) \right|^{p^\mathfrak{D}(x)}.$$

Then (21) and (20) yield

$$\|\nabla^\mathfrak{D} u^\mathfrak{T}\|_{L^{p_-}}^{p_-} \leq |\Omega| + \rho_{p^\mathfrak{D}(\cdot)}(\nabla^\mathfrak{D} u^\mathfrak{T}) \leq \text{const} \left(1 + \|f\|_{L^{p'_-(\Omega)}} \|\nabla^\mathfrak{D} u^\mathfrak{T}\|_{L^{p_-}} \right).$$

Because $p_- > 1$, this permits to bound $\|\nabla^\mathfrak{D} u^\mathfrak{T}\|_{L^{p_-}}$ and then, by using (21) and (20) again, we reach to (22). By Proposition 1.2, the bound (22) further entails a uniform bound on $\|\nabla^\mathfrak{D} u^\mathfrak{T}\|_{L^{p^\mathfrak{D}(\cdot)}(\Omega)}$.

For a fixed mesh \mathfrak{T} , this norm is equivalent to any standard norm of $u^\mathfrak{T}$ on the finite-dimensional space $\mathbb{R}^\mathfrak{T}$. The resulting *a priori* bound guarantees the existence of a solution to (17), based either upon the Brouwer fixed-point theorem or upon the topological degree argument (cf. [10, 35, 38, 47]).

In the sequel, we extract convergent subsequences from the family $(\mathfrak{T}_n)_n$ without labeling them (as a shortcut, we write “convergence, as $\text{size}(\mathfrak{T}) \rightarrow 0$ ”). At the end of the proof, as soon as the convergence (up to a subsequence) of discrete solutions to a weak solution of the continuous problem is established, the standard result of uniqueness of a weak solution to (1), (2) permits to assess that the whole sequence converges.

Step 2. We apply the discrete W_0^{1,p_-} compactness results proper to each scheme, e.g., for the DDFV scheme we use [10, Lemma 3.8]². More precisely, the uniform bounds of Step 1, the fact that $p^\mathfrak{D} \geq p_-$ (see (16)) and the Poincaré–Friedrichs inequality for $q = p_-$ entail the strong convergence of $u^\mathfrak{T}$ in $L^{p_-}(\Omega)$ to some limit that we denote u ; furthermore, they entail the weak convergence of $\nabla^\mathfrak{D} u^\mathfrak{T}$ in $(L^{p_-}(\Omega))^2$ to some limit that we denote \mathcal{G} , whereas property (12) ensures that $\mathcal{G} = \nabla u$. We deduce in particular that $u \in W_0^{1,1}(\Omega)$ (and even in $W_0^{1,p_-}(\Omega)$).

Step 3. The energy estimate (22) entails the boundedness of the family $\mathfrak{a}^\mathfrak{D}(\cdot, \nabla^\mathfrak{D} u^\mathfrak{T})$ in $(L^{\frac{p_+}{p_+ - 1}}(\Omega))^2$, since $|\mathfrak{a}^\mathfrak{D}(\cdot, \xi)|^{\frac{p_+}{p_+ - 1}} = |\xi|^{p_+}$ and $\frac{p_+}{p_+ - 1} \geq \frac{p_+}{p_+ - 1}$ in view of (16). By the De La Vallée Poussin equi-integrability property and the Dunford–Pettis characterization of the weak convergence in L^1 spaces, $\mathfrak{a}^\mathfrak{D}(\cdot, \nabla^\mathfrak{D} u^\mathfrak{T})$ converges weakly in $(L^1(\Omega))^2$ (up to a subsequence), as $\text{size}(\mathfrak{T}) \rightarrow 0$, to some limit we denote χ .

Step 4. Then the standard argument (see, e.g., the first step of the proof of [10, Theorem 5.1]) permits to pass to the limit, as $\text{size}(\mathfrak{T}) \rightarrow 0$, in the scheme (17). More precisely, this is done taking as the discrete test function a straightforward discretization $\phi^\mathfrak{T}$ of a fixed

²As in [10, Theorem 5.1], for the DDFV context the proof of strong convergence of $u^\mathfrak{T}$ requires two steps: until the identification of the limit, one only needs that $u^{\mathfrak{M}^n}, u^{\mathfrak{M}^k}$ strongly converge the some limits u_{primal} and u_{dual} respectively, and sets $u := (u_{\text{primal}} + u_{\text{dual}})/2$; and at the very end of the proof, using the Poincaré inequality (we can again stick to the constant exponent case $q = p_-$) one finds that $u_{\text{primal}} = u_{\text{dual}} = u$. For more involved PDE problems, e.g., those involving nonlinear reaction terms, one may need to penalize the difference $u^{\mathfrak{M}^n} - u^{\mathfrak{M}^k}$ in order to ensure that $u_{\text{primal}} = u_{\text{dual}} = u$ at the limit (see [4, 6]).

smooth test function ϕ . In this situation, $\nabla^{\mathfrak{D}^n} \phi^{\overline{\mathfrak{X}}}$ converges a.e. on Ω and strongly in all L^q spaces towards $\nabla \phi$ (the property (11)), while $\phi^{\mathfrak{X}}$ converges a.e. on Ω and strongly in all L^q spaces towards ϕ (in the DDFV context, each of the two components $\phi^{\mathfrak{M}^n}$, $\phi^{\mathfrak{M}^{n*}}$ converges strongly to the same limit ϕ) in the sense (10). The weak convergence obtained in Step 3, the expression (8) and (11) show that the left-hand side of (17) converges to the left-hand side of the identity

$$\int_{\Omega} \chi(x) \cdot \nabla \phi(x) \, dx = \int_{\Omega} f(x) \phi(x) \, dx \tag{23}$$

as $\text{size}(\overline{\mathfrak{X}}) \rightarrow 0$. At the same time, the right-hand side of (17) converges to the right-hand side of (23) due to (10). Consequently, the relation (23) linking χ and u is valid for all test function $\phi \in C_0^\infty(\Omega)$.

The remainder of the proof consists in showing that $u \in \mathbf{W} = \mathbf{H}$ and $\chi = \mathfrak{a}(\cdot, \nabla u)$, which is done based on the Young measure representation of ∇u and χ and the monotonicity of \mathfrak{a} .

Step 5. We start by applying Theorem 3 to express ∇u and χ via the same Young measure, the one generated by (a subsequence of) $(\nabla^{\mathfrak{D}} u^{\overline{\mathfrak{X}}})$. Indeed, notice that the (log-Hölder) continuity of $p(\cdot)$ and the choice (16) ensure the uniform on $\overline{\Omega}$ convergence of $p^{\mathfrak{D}}(\cdot)$ to $p(\cdot)$, in particular Theorem 3(ii) tells us that the Young measure generated by the family $(p^{\mathfrak{D}})$ (remember we skip the labeling of meshes by n to lighten the notation) is $\delta_{p(x)}$. By Theorem 3(i), $\nabla u = \mathcal{G}$ being the weak L^1 limit of the family of $(L^1(\Omega))^2$ functions $(\nabla^{\mathfrak{D}} u^{\overline{\mathfrak{X}}}(\cdot))$, it can be represented by the Young measure we denote $d\nu_x$:

$$\nabla u(x) := \int_{\mathbb{R}^2} \xi \, d\nu_x(\xi). \tag{24}$$

From these two claims it follows by Theorem 3(iii) that the Young measure representing the family $(p^{\mathfrak{D}}(\cdot), \nabla^{\mathfrak{D}} u^{\overline{\mathfrak{X}}}(\cdot))$ is $\delta_{p(x)} \otimes \nu_x$. Now, we apply formula (14) of Theorem 3 for the latter family, with the choice $F(\pi, \xi) = |\xi|^{\pi-2} \xi$. Note that the discrete flux $\mathfrak{a}^{\mathfrak{D}}(\cdot, \nabla^{\mathfrak{D}} u^{\overline{\mathfrak{X}}}(\cdot))$ writes as $F(p^{\mathfrak{D}}(\cdot), \nabla^{\mathfrak{D}} u^{\overline{\mathfrak{X}}}(\cdot))$, and the $(L^{\frac{p_+}{p_+ - 1}}(\Omega))^2$ estimate of Step 3 ensures the equi-integrability of $F(p^{\mathfrak{D}}(\cdot), \nabla^{\mathfrak{D}} u^{\overline{\mathfrak{X}}}(\cdot))$ required in Theorem 3(i). This permits to write

$$\chi(x) := \int_{\mathbb{R}^2} F(\pi, \xi) \, d\delta_{p(x)}(\pi) \otimes \nu_x(\xi) = \int_{\mathbb{R}^2} |\xi|^{p(x)-2} \xi \, d\nu_x(\xi). \tag{25}$$

Step 6. Next, we prove that $u \in \mathbf{W}$; in view of the definition of \mathbf{W} and the result of Step 2, it remains to prove that $\nabla u \in (L^{p(\cdot)}(\Omega))^2$ due to the uniform bound (22). We employ a simple semi-continuity argument, which we detail for the sake of completeness. Introduce, for $m > 0$, the truncations

$$h_m : \mathbb{R}^2 \longrightarrow \mathbb{R}^2, \quad h_m(\xi) = \begin{cases} \xi, & |\xi| \leq m, \\ m \frac{\xi}{|\xi|}, & |\xi| > m. \end{cases} \tag{26}$$

Because $h_m(\cdot)$ is bounded for every fixed m , we can apply Theorem 3(i),(iii) with the function $F_m(\pi, \xi) = |h_m(\xi)|^\pi$ to the sequence $(p^{\mathfrak{D}}(\cdot), \nabla^{\mathfrak{D}} u^{\overline{\mathfrak{X}}}(\cdot))$ (cf. Step 5). We find for all $m < \infty$,

$$\int_{\Omega} \int_{\mathbb{R}^2} F_m(\pi, \xi) \, d\delta_{p(x)}(\pi) \otimes \nu_x(\xi) \, dx = \lim_{\text{size}(\overline{\mathfrak{X}}) \rightarrow 0} \int_{\Omega} F_m \left(p^{\mathfrak{D}}(x), \nabla^{\mathfrak{D}} u^{\overline{\mathfrak{X}}}(x) \right) \, dx. \tag{27}$$

The right-hand side of (27) is upper bounded by

$$\int_{\Omega} F\left(p^{\mathfrak{D}}(x), \nabla^{\mathfrak{D}} u^{\overline{\mathfrak{T}}}(x)\right) dx = \int_{\Omega} \left|\nabla^{\mathfrak{D}} u^{\overline{\mathfrak{T}}}(x)\right|^{p^{\mathfrak{D}}(x)} dx = \rho_{p^{\mathfrak{D}}(\cdot)}(\nabla^{\mathfrak{D}} u^{\overline{\mathfrak{T}}}),$$

where we used the fact that $F_m(\cdot, \cdot) \leq F(\cdot, \cdot)$ pointwise since $|h_m(\cdot)| \leq |\cdot|$. Whence by (22), the right-hand side of (27) is bounded uniformly with respect to m . To conclude, observe that $|h_m(\cdot)|^{p(x)} \rightarrow |\cdot|^{p(x)}$, as $m \rightarrow \infty$, moreover, the convergence is monotone. We then have

$$\int_{\Omega} \int_{\mathbb{R}^2} |\xi|^{p(x)} d\nu_x(\xi) dx = \lim_{m \rightarrow \infty} \int_{\Omega} \int_{\mathbb{R}^2} F_m(\pi, \lambda) d\nu_x(\xi) dx$$

so that $(\xi, x) \mapsto |\xi|^{p(x)}$ is integrable with respect to the measure $d\nu_x(\xi) dx$. Finally, in view of the representation (24) and due to the convexity of $\xi \mapsto |\xi|^{p(x)}$, by the Jensen inequality we deduce that ∇u belongs to $L^{p(\cdot)}$.

Moreover, in a very similar manner we find that $\chi \in L^{p'(\cdot)}$ due to the representation (25), the convexity of $\xi \mapsto |\xi|^{p'(x)}$, and the Jensen inequality.

Step 7. The key assumption (3) on $p(\cdot)$ ensures that $\mathbf{W} = \mathbf{H}$ and therefore, $u \in \mathbf{H}$ is an admissible test function in the weak formulation. Indeed, $u \in \mathbf{H}$ can be approximated in the norm of $W^{1,p(\cdot)}(\Omega)$ by $C_c^\infty(\Omega)$ functions; in view of the $L^{p'(\cdot)}(\Omega)$ integrability of χ and the assumption $f \in L^{(p-)'(\cdot)}(\Omega) \subset L^{p'(\cdot)}(\Omega)$, the density argument permits to extend the validity of (23) to the choice $\phi = u$.

At the same time, we can take the test function $u^{\overline{\mathfrak{T}}}$ in the discrete weak formulation (17). Having in mind property (10) (applied with the constant exponent $(p_-)'$, due to the assumption $f \in L^{(p-)'(\cdot)}(\Omega)$), this yields

$$\begin{aligned} \int_{\Omega} \chi(x) \cdot \nabla u(x) dx &= \int_{\Omega} f(x)u(x) dx = \lim_{\text{size}(\mathfrak{T}) \rightarrow 0} \left[f^{\overline{\mathfrak{T}}}, u^{\overline{\mathfrak{T}}} \right] \\ &= \lim_{\text{size}(\mathfrak{T}) \rightarrow 0} \left\{ \alpha^{\mathfrak{D}}(\cdot, \nabla^{\mathfrak{D}} u^{\overline{\mathfrak{T}}}), \nabla^{\mathfrak{D}} u^{\overline{\mathfrak{T}}} \right\} \\ &= \lim_{\text{size}(\mathfrak{T}) \rightarrow 0} \int_{\Omega} \left| \nabla^{\mathfrak{D}} u^{\overline{\mathfrak{T}}}(x) \right|^{p^{\mathfrak{D}}(x)} dx. \end{aligned} \tag{28}$$

We can rewrite the left-hand side of (28), using (24) and (25), as

$$\int_{\Omega} \left(\int_{\mathbb{R}^2} \xi d\nu_x(\xi) \right) \cdot \left(\int_{\mathbb{R}^2} |\xi|^{p(x)} d\nu_x(\xi) \right) dx.$$

Step 8. The above inequality allows us to reduce the Young measure ν_x to the Dirac measure $\delta_{\nabla u(x)}$ and to identify $\chi(x)$ with $\alpha(x, \nabla u(x))$.

While one cannot apply Theorem 3 to represent this limit because the equi-integrability property fails, a lower semi-continuity argument similar to the one detailed in Step 6 applies. First, for every fixed $m < \infty$ we can lower bound the right-hand side of (28) by

$$\lim_{\text{size}(\mathfrak{T}) \rightarrow 0} \int_{\Omega} \left| h_m(\nabla^{\mathfrak{D}} u^{\overline{\mathfrak{T}}}(x)) \right|^{p^{\mathfrak{D}}(x)} dx = \int_{\mathbb{R}^2} |h_m(\xi)|^{p(x)} \xi d\nu_x(\xi).$$

Then we let $m \rightarrow \infty$ using the monotone convergence theorem, thus reaching to

$$\int_{\Omega} \left(\int_{\mathbb{R}^2} \xi d\nu_x(\xi) \right) \cdot \left(\int_{\mathbb{R}^2} |\xi|^{p(x)-2} \xi d\nu_x(\xi) \right) dx \geq \int_{\Omega} \int_{\mathbb{R}^2} (\xi) \cdot (|\xi|^{p(x)-2} \xi) d\nu_x(\xi) dx.$$

As in [7, 33, 45], elementary manipulations based on the fact that ν_x is a probability measure on \mathbb{R}^2 lead to

$$0 \geq \int_{\Omega} \int_{\mathbb{R}^2} \int_{\mathbb{R}^2} (\xi - \zeta) \cdot \left(|\xi|^{p(x)-2} \xi - |\zeta|^{p(x)-2} \zeta \right) d\nu_x(\xi) d\nu_x(\zeta) dx. \tag{29}$$

The monotonicity of the map $\xi \mapsto |\xi|^{p(x)-2} \xi$ entails that the integrand in (29) is nonnegative; whence

$$\begin{aligned} (\xi - \zeta) \cdot \left(|\xi|^{p(x)-2} \xi - |\zeta|^{p(x)-2} \zeta \right) &= 0 \\ \text{a.e. on } \mathbb{R}^2 \times \mathbb{R}^2 \times \Omega &\text{ with respect to } d\nu_x(\xi) d\nu_x(\zeta) dx. \end{aligned}$$

Since the above mentioned monotonicity is strict, this actually means that $\nu_x(\xi) \otimes \nu_x(\zeta)$ -a.e., $\xi = \zeta$ for a.e. $x \in \Omega$. This forces ν_x to be a Dirac measure on \mathbb{R}^2 , whence by (24) we have $\nu_x = \delta_{\nabla u(x)}$ and then by (25), $\chi(x) = |\nabla u(x)|^{p(x)-2} \nabla u(x) = \alpha(x, \nabla u(x))$ for a.e. $x \in \Omega$.

This concludes the proof of identification of χ . Inserting it into (23), we conclude that u constructed in Step 1 is a solution of (1), (2) in the sense of Definition 2.

Step 9. It remains to prove the strong convergences claimed in (18) and in (19); they are byproducts of the above proof. It follows from Step 1 that $u^{\mathfrak{T}} \rightarrow u$ in $L^1(\Omega)$ while it follows from Step 8 and Theorem 3(ii) that $\nabla^{\mathfrak{D}} u^{\mathfrak{T}} \rightarrow \nabla u$ in measure, as $\text{size}(\mathfrak{T}) \rightarrow 0$; thus upon extraction of a further subsequence, (18) holds. Next, we revisit (28) by rewriting the left-hand side of it using the representation of χ . We reach to

$$\int_{\Omega} |\nabla u(x)|^{p(x)} dx = \lim_{\text{size}(\mathfrak{T}) \rightarrow 0} \int_{\Omega} \left| \nabla^{\mathfrak{D}} u^{\mathfrak{T}}(x) \right|^{p^{\mathfrak{D}}(x)} dx,$$

bearing in mind that $|\nabla^{\mathfrak{D}} u^{\mathfrak{T}}(x)|^{p^{\mathfrak{D}}(x)} \rightarrow |\nabla u(x)|^{p(x)}$ due to (18) and to the obvious convergence of discretizations $p^{\mathfrak{D}}$. The claim (19) follows by the refinement of the Fatou lemma, sometimes referred to as the Schaeffe’s lemma (cf. [35, Lemma 8.4]). \square

Remark 1 The particular form (2) of the variable-exponent nonlinearity α is strongly exploited in the above proof. Adaptation of the proof to more general Leray–Lions kind nonlinearities, under the assumptions of [7], is not difficult but some of the arguments become more technical. In this relation, note that in the context of Theorem 4, we have the uniform convergence of $p^{\mathfrak{D}}$ to $p(\cdot)$ and therefore, in the context of Step 3 of the above proof, the heavy cutting argument of [7, Claim 7] can be bypassed.

3.2 Adaptation to the $p(u)$ -Laplacian

The result of Theorem 4 admits a simple extension to the situation where the nonlinearity α in (1) and the variable exponent $p(\cdot)$ are allowed to depend on the solution u . For the sake of simplicity, here we only consider the $p(u)$ -laplacian situation with (2) replaced by

$$\alpha(x, u, \nabla u) = |\nabla u|^{\sigma(x, u(x))-2} \nabla u, \quad \sigma : \Omega \times \mathbb{R} \longrightarrow (1, \infty)$$

With a slight abuse of notation, we refer to the associated Dirichlet problem as “problem (1), (2) with $p(\cdot) = \sigma(\cdot, u(\cdot))$ ”. In [8], it was shown that the stability technique of [7] readily extends to this case under a set of assumptions ensuring the log-Hölder regularity of the resulting exponent $p(\cdot)$. To this end, we are led to assume

$$\sigma \text{ extends to a Hölder continuous function on } \overline{\Omega} \times \mathbb{R}, \tag{30}$$

$$\sigma \text{ takes values in } [p_-, p_+] \text{ with } p_- > d, \tag{31}$$

where we recall that d is the space dimension. The associated well-posedness theory is constructed in [8]. Note that for the uniqueness, additional assumptions are required on σ . If we assume only (30), (31), then the following analogue of Theorem 4 holds up to extraction of a subsequence (and without extraction of a subsequence, under additional assumptions of [8] ensuring the uniqueness for the $p(u)$ -laplacian problem at hand).

Theorem 5 *In the context of the assumptions of Theorem 4, consider the problem (1), (2) with $p(\cdot) = \sigma(\cdot, u(\cdot))$ with σ satisfying (30), (31). For the DDFV case, consider in the place of (17) the penalized scheme of [4, 6] using the constant exponent $q = p_-$ in the definition of the penalization operator.*

Regarding the discretization $p^{\mathfrak{D}_n} = (p_D)_{D \in \mathfrak{D}_n} \in \mathbb{R}^{\mathfrak{D}_n}$ of the variable exponent $p(\cdot) = \sigma(\cdot, u(\cdot))$ on the diamond mesh, we assume that for each $D \in \mathfrak{D}_n$, $p_D \in [p_-, p_+]$ is chosen so that

$$\min_{K \in \mathcal{V}(D)} \sigma(x_K, u_K) \leq p_D \leq \max_{K \in \mathcal{V}(D)} \sigma(x_K, u_K), \tag{32}$$

where $\mathcal{V}(D)$ denotes the set of all control volumes $K \in \mathfrak{T}_n$ (both primal and dual ones, in the DDFV setting) which centers are vertices of the diamond $D \in \mathfrak{D}_n$.

Then, up to extraction of a subsequence, the conclusion of Theorem 4 on convergence to a limit u —solution of (1), (2) with $p(\cdot) = \sigma(\cdot, u(\cdot))$ —hold true.

Proof This is a straightforward adaptation of the proof of Theorem 4.

We focus on the fact that $p^{\mathfrak{D}}$ converges to the limit $\sigma(\cdot, u(\cdot))$ where u is the strong limit of $u^{\mathfrak{T}}$ in $L^{p^-}(\Omega)$. At this point, the penalization of [6], see also [4], is needed in the DDFV framework in order to ensure that $u^{\mathfrak{M}^*} - u^{\mathfrak{M}^*}$ converges to zero strongly in $L^{p^-}(\Omega)$. The estimate of Step 1 ensures that whatever be the choice of $K_D \in \mathcal{V}(D)$ for each $D \in \mathfrak{D}$, the discrete functions $\sum_{D \in \mathfrak{D}} u_{K_D} \mathbb{1}_D$ converge to the same limit u , as $\text{size}(\mathfrak{T}) \rightarrow 0$. Then the uniform continuity of σ (which is a consequence of (30)) ensures that under the assumption (32), we do have the strong a.e. convergence $p^{\mathfrak{D}} \rightarrow \sigma(\cdot, u(\cdot)) =: p(\cdot)$. This allows us applying Theorem 3(iii) in the context of Steps 5, 6 and 8 of the proof of Theorem 4.

The other key argument is the property $\mathbf{W} = \mathbf{H}$ underlying Step 7; it is readily deduced from (30) and from the restriction (31) ensuring that u is Hölder continuous on $\overline{\Omega}$ due to the Gagliardo–Sobolev embedding.

The other steps of the proof are unchanged in the CVFE context. To handle the introduction—in the DDFV context—of penalization within the scheme (17), note that it corresponds to the addition of a discrete term corresponding to $-\text{size}(\mathfrak{T}) \Delta_{p_-} u$ in the left-hand side of (17). This term permits to replace (28) with the inequality “ \geq ” (which is typical of the monotonicity arguments of the Minty–Browder kind and compatible with our Young-measure-based argument), moreover this penalization term vanishes from the weak formulation as $\text{size}(\mathfrak{T}) \rightarrow 0$ due to the straightforward *a priori* estimate obtained as in [4, 6]. The same *a priori* estimate is exploited for the proof of existence of a discrete solution. We refer to [4] for details on these issues. □

3.3 Extensions to $p[u]$ -Laplacian and Evolution Problems

Without giving precise statements and entering the detailed analysis, let us point out that in a very similar way, one could deal with problems where $p(\cdot)$ depends on u nonlocally, typically $p(\cdot) = \sigma(\cdot, v(\cdot))$ where $v(\cdot)$ satisfies a PDE with $u(\cdot)$ -dependent coefficients. Such coupled problems naturally appear in applications, see e.g. [14, 56]. We token this vast

family of problems as $p[u]$ -laplacian variable exponent problems. A sample situation was treated in detail in [8]; the key assumption, for the adaptation of the convergence technique we pursue here, is the (log-)Hölder regularity of the resulting exponent $p(\cdot)$.

It is also possible to exploit the analysis technique of Theorem 4 in the context of evolution problems of $p(x)$, $p(u)$ or $p[u]$ -laplacian kind, under the general form $u_t - \operatorname{div} a(t, x, \nabla u) = 0$ with (t, x) -dependent variable exponent $p(\cdot)$ which may depend on $u(\cdot)$ in a local or in a non-local way. This requires adaptation to the functional framework established for the evolution problem, see, e.g. [15, 22, 31], and in particular the chain rule / integration-by-parts argument, known as the Mignot–Bamberger or Alt–Luckhaus lemma, is required in Step 7 of the proof (cf. [22]).

We do not pursue here any of these lines in our analysis, but we provide below a numerical test corresponding to a particular instance of $p[u]$ -laplacian stationary problem borrowed from [56].

3.4 Numerical Experiments

This subsection is devoted to exhibiting the behavior of the CVFE scheme with respect to various nonlinearities spanned by smooth formulas of the exponent in the $p(\cdot)$ -Laplacian problem. In this case, the \mathbf{H} -solution and the \mathbf{W} -solution (see Definition 3) are identical.

The domain of computation is fixed to $\Omega = (-1, 1)^2$. It is discretized using a regular family of triangulations. Each triangular mesh, indexed by ℓ where $1 \leq \ell \leq 6$, is obtained by decomposing the squares of the Cartesian mesh, made from $2^{1+\ell} \times 2^{1+\ell}$ cells, into triangles along their diagonals. Figure 2 illustrates the first two elements of the primal mesh. The proposed finite volume scheme yields a nonlinear algebraic system solved thanks to the Newton–Raphson’s algorithm. Its tolerance is fixed to $\varepsilon = 10^{-8}$. The stopping criterion is applied on the relative error of the successive iterates in the sense of $\|\cdot\|_\infty$ -norm.

In all the numerical examples below, the exact solution is unknown. Then, we are led to consider a reference solution on a very refined mesh of level $\ell = 7$ in order to assess the accuracy of the finite volume scheme. Quantifying the errors requires the introduction of the following approximate modular

$$Q_{p(\cdot)}(u_{\text{ref}} - u_h) = \int_{\Omega} |u_{\text{ref}} - u_h|^{\tilde{p}_h(x, u_h)} dx,$$

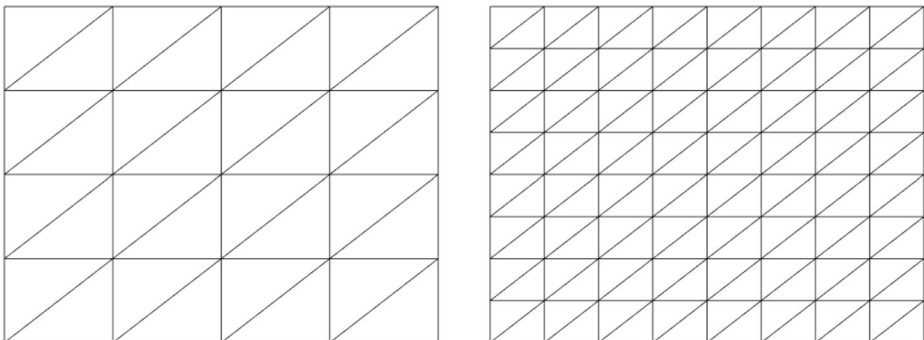


Fig. 2 The first and the second triangulations of Ω

where \tilde{p}_h is a piecewise constant approximation of $p(\cdot)$ on the triangulation of Ω . Precisely, let S_1, S_2, S_3 denote the vertices of the triangle D , the expression of \tilde{p}_h is given by

$$\tilde{p}_h(x, u_h) = \frac{p(x_{S_1}, u_1) + p(x_{S_2}, u_2) + p(x_{S_3}, u_3)}{3}, \quad \forall x \in D, \forall D \in \mathcal{T}_h;$$

note that it satisfies (16). The number $\varrho_{p(\cdot)}$ entails no information on the accuracy, nor on the convergence speed, but it enables the computation of Luxemburg’s norm written as

$$\|u_{\text{ref}} - u_h\|_{p(\cdot)} = \inf \left\{ \lambda > 0, \varrho_{p(\cdot)} \left(\frac{u_{\text{ref}} - u_h}{\lambda} \right) \leq 1 \right\}.$$

The function $g : \lambda \rightarrow \varrho_{p(\cdot)}((u_{\text{ref}} - u_h)/\lambda) - 1$ being decreasing, a dichotomy routine is implemented to compute $\|u_{\text{ref}} - u_h\|_{p(\cdot)}$. Before that, we need to determine an interval, whose extremities are λ_0, λ_1 , for which $g(\lambda_0)g(\lambda_1) < 0$. For this purpose, it suffices to choose a value of λ_0 , retain its sign and deduce the other one by dividing (resp. multiplying) its by 1/2 (resp. by 2) until the opposite sign is reached.

A similar approach is adopted to calculate the errors of the gradients. In the tables of the sequel, the notations $\text{Rho}_u, \text{Err}_u, \text{Rho}_{gu}, \text{Err}_{gu}$ refer respectively to the quantities

$$\varrho_{p(\cdot)}(u_{\text{ref}} - u_h), \quad \|u_{\text{ref}} - u_h\|_{p(\cdot)}, \quad \varrho_{p(\cdot)} \left(\nabla_h^{\text{ref}} u_{\text{ref}} - \nabla_h u_h \right), \quad \left\| \nabla_h^{\text{ref}} u_{\text{ref}} - \nabla_h u_h \right\|_{p(\cdot)}.$$

3.4.1 Test 1

The goal of this first experiment is to validate the scheme and to test its accuracy in the case where the variable exponent $p(\cdot)$ is only depending on space, in a smooth way. We then consider for $x = (x_1, x_2) \in \mathbb{R}^2$

$$p(x) = \frac{5}{2} + \cos(x_1) \cos(x_2).$$

We take a constant right-hand side as $f(x) = 10$. A homogeneous Dirichlet boundary condition is prescribed. The numerical convergence results are shown in Table 1. A second order accuracy is obtained for the solution and an accuracy of order around 3/2 for the gradients, in the Luxemburg norm. This is expected because of the data smoothness. Figure 3 illustrates the 2D view of the numerical solution on the third mesh.

Table 1 Numerical convergence for Test 1

h	Rho_u	Err_u	rate	Rho_{gu}	Err_{gu}	rate
0.354E+00	0.130E-01	0.129E+00	-	0.960E-01	0.317E+00	-
0.177E+00	0.152E-02	0.396E-01	1.699	0.176E-01	0.396E-01	1.384
0.884E-01	0.123E-03	0.104E-01	1.926	0.190E-02	0.104E-01	1.692
0.442E-01	0.906E-05	0.261E-02	1.996	0.174E-03	0.261E-02	1.598
0.221E-01	0.626E-06	0.625E-03	2.064	0.144E-04	0.625E-03	1.481
0.110E-01	0.322E-07	0.125E-03	2.322	0.876E-06	0.125E-03	1.678

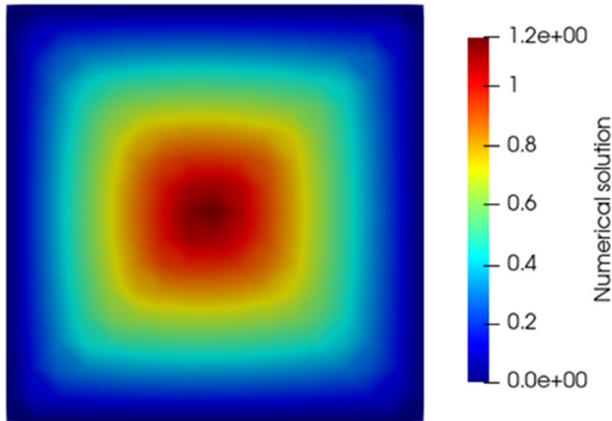


Fig. 3 Test 1: numerical solution on the third mesh

3.4.2 Test 2

In this second example, we are interested in the case where the exponent function depends nonlinearly on the solution itself such as

$$p(x) = \sigma(x, u(x)) = \frac{5}{2} + \arctan(u(x)).$$

We also consider the following right-hand side defined by

$$f(x) = 100 \frac{2x_1 + x_2}{x_1^2 + 3x_2^2 + 1}.$$

The Dirichlet boundary conditions are non-homogeneous (note that the extension of the convergence analysis of Theorem 4 to the inhomogenous Dirichlet conditions can be obtained as in [10], at least when the boundary condition is the trace of a $W^{1,p+}(\Omega)$ function) and they are prescribed by the function

$$u(x) = (x_1 - 0.5)^2 + (x_2 - 0.5)^2, \quad \forall x = (x_1, x_2) \in \partial\Omega.$$

The results on the convergence rates are displayed in Table 2. A small loss of convergence is recorded on the first two meshes, while the second order accuracy is recovered as the mesh is refined. However, only a linear rate is noticed for the gradients. Thus the dependency of the variable exponent on the solution impacts the accuracy. Figure 4 indicates how the shape

Table 2 Numerical convergence for Test 2

h	Rho_u	Err_u	rate	Rho_gu	Err_gu	rate
0.354E+00	0.684E-03	0.120E+00	-	0.441E-01	0.412E+00	-
0.177E+00	0.263E-04	0.491E-01	1.286	0.171E-01	0.491E-01	0.353
0.884E-01	0.460E-06	0.154E-01	1.676	0.757E-03	0.154E-01	1.275
0.442E-01	0.244E-08	0.362E-02	2.086	0.718E-04	0.362E-02	0.931
0.221E-01	0.332E-10	0.100E-02	1.852	0.854E-05	0.100E-02	0.833
0.110E-01	0.262E-12	0.255E-03	1.977	0.830E-06	0.255E-03	0.950

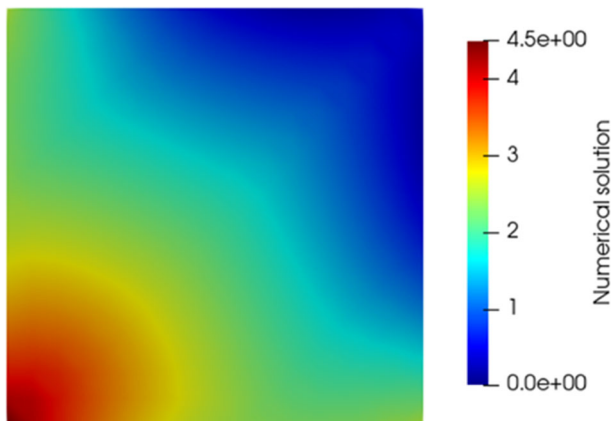


Fig. 4 Test 2: numerical solution on the third mesh

of the obtained solution looks on the third triangular mesh. We plot in Fig. 5 the behavior of the approximate solution to the above problem.

3.4.3 Test 3

We here look at the situation where the exponent solves an elliptic equation. The right-hand side of the latter is given under the form of Joule heating term with a variable exponent. This system, taken from [56], is a generalization of the well-known steady thermistor problem. It reads

$$\begin{cases} -\operatorname{div} (|\nabla u|^{\sigma(\theta)-2} \nabla u) = f, & u|_{\partial\Omega} = 0, \\ -\Delta \theta = \alpha |\nabla u|^{\sigma(\theta)}, & \theta|_{\partial\Omega} = 0, \quad \alpha > 0, \end{cases}$$

where we take

$$\sigma(\theta) = \frac{5}{2} + \frac{2}{\pi} \arctan(\theta), \quad f(x) = 4((1 - x_1)(x_1 + 1) + (1 - x_2)(x_2 + 1)), \quad \alpha = 0.5.$$

The errors and their convergence rates are shown in Table 3 for u . Similar outcomes are obtained as in the first example. Table 4 gives the errors together with the orders with respect to θ . The results are computed in the sense of the L^2 norm for the solution and its gradient. In both cases, a quadratic convergence is reached. This is standard and is due to the fact that the mesh is structured.

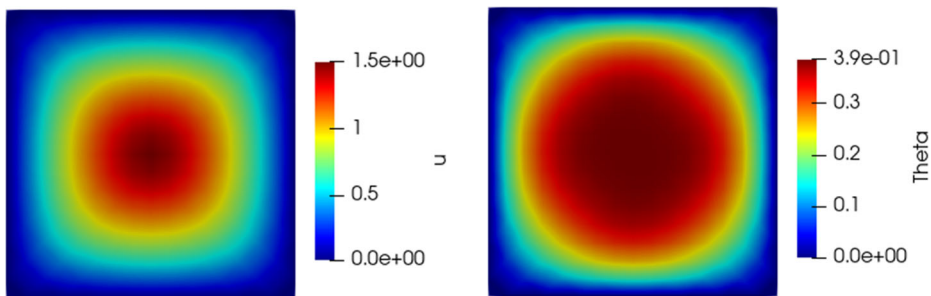


Fig. 5 Test 3: (left) behavior of u (right) and θ (left) on the third mesh

Table 3 Numerical convergence for Test 3 with respect to u

h	Rho_ u	Err_ u	rate	Rho_ gu	Err_ gu	rate
0.354E+00	0.253E-04	0.188E-01	-	0.160E-02	0.911E-01	-
0.177E+00	0.836E-06	0.531E-02	1.826	0.168E-03	0.531E-02	1.198
0.884E-01	0.236E-07	0.139E-02	1.930	0.131E-04	0.139E-02	1.366
0.442E-01	0.637E-09	0.356E-03	1.970	0.915E-06	0.356E-03	1.420
0.221E-01	0.152E-10	0.849E-04	2.067	0.561E-07	0.849E-04	1.479
0.110E-01	0.227E-12	0.181E-04	2.228	0.198E-08	0.181E-04	1.774

Although we do not pursue this line in this paper, note that the scheme readily extends to evolution problem with the CVFE strategy developed for a different version of the generalized thermistor problem in [42]; both numerical tests and convergence analysis in the evolution framework are left for future work.

4 The Lavrentiev Phenomenon: Approximation of Broad and Narrow Solutions

The proof of Theorem 4 requires, at Step 7, that the limit $u \in \mathbf{W}$ be taken as a test function in the equation (23); while the standard approach of consistency of the Finite Volume scheme with the weak formulation ensures that any $\phi \in C_c^\infty(\Omega)$ (and then, by density, $\phi \in \mathbf{H}$) is an admissible test function. In this context, the log-Hölder regularity assumption (3) on $p(\cdot)$ is imposed in order to ensure that $\mathbf{W} = \mathbf{H}$ while in general, one may have $\mathbf{H} \subsetneq \mathbf{W}$; e.g. for (4) the inclusion is indeed strict. Therefore in general, one should distinguish two notions of weak solution generalizing Definition 2. In the remaining part of this section, we drop the log-Hölder assumption on the variable exponent $p(\cdot)$.

Definition 3 (cf. [7]) Assume $p(\cdot)$ is measurable and $f \in L^{(p^*)'(\cdot)}(\Omega)$. A narrow weak solution of the homogeneous Dirichlet $p(x)$ -laplacian problem (1), (2) is a function u that fulfills the analogue of (15) with $u, \phi \in \mathbf{H}$. A broad weak solution of the same problem is a function u that fulfills the analogue of (15) with $u, \phi \in \mathbf{W}$.

A common terminology in the literature devoted to the Lavrentiev phenomenon is to call the above solution notions “ \mathbf{H} -solution” and “ \mathbf{W} -solution”, respectively.

Table 4 Numerical convergence for Test 3 with respect to θ

h	ErrL2_ θ	rate	ErrL2_ $g\theta$	rate
0.354E+00	0.341E-01	-	0.138E+00	-
0.177E+00	0.122E-01	1.479	0.568E-01	1.285
0.884E-01	0.325E-02	1.912	0.158E-01	1.841
0.442E-01	0.813E-03	2.000	0.402E-02	1.977
0.221E-01	0.194E-03	2.068	0.964E-03	2.061
0.110E-01	0.388E-04	2.322	0.193E-03	2.320

Note that for each of these notions of solution uniqueness is straightforward, while existence can be inferred using the stability technique highlighted in this paper (see [7, Theorem 3.11]; our assumption $f \in L^{(p^*)'(\cdot)}(\Omega)$ ensures that the renormalized broad (respectively, renormalized narrow) solution constructed in [7] is also a narrow weak (resp., broad weak) solution). In general, the two solutions may differ, which is known, in the variational interpretation of our PDE problem, as the Lavrentiev phenomenon. In [7, 59], it is demonstrated, moreover, that for problems including (1), (2)

- a sequence of narrow solutions with $p_n(\cdot) \rightarrow p(\cdot)$, $p_n \geq p$ a.e. in Ω , converges to a narrow solution;
- a sequence of broad solutions with $p_n(\cdot) \rightarrow p(\cdot)$, $p_n \leq p$ a.e. in Ω , converges to a broad solution.

In the context of numerical approximations, we have two alternative ways to proceed, for proving convergence to one or the other type of weak solution:

- either ensure that the limit u of $u^{\mathfrak{T}}$ belongs to the narrow space \mathbf{H} while the proof in Step 6 gives us only the weaker property $u \in \mathbf{W}$ (in this case, the scheme would approximate the narrow weak solution);
- or ensure that the limit equation (23) holds with test functions $\phi \in \mathbf{W}$ while the standard approximation properties of the CVFE and DDFV schemes only yield it with smooth test functions ϕ and, by density, for $\phi \in \mathbf{H}$ (in this case, the scheme would approximate the broad weak solution).

Heading towards convergence analysis, we borrow from [7] (and from Zhikov [59]) the assumption $p^{\mathfrak{D}^n} \geq p(\cdot)$ for reaching the narrow solution, and the assumption $p^{\mathfrak{D}^n} \leq p(\cdot)$ for reaching the broad solution of our problem. Moreover, we get insight from the analysis, in [17], of convergence of conforming and non-conforming Finite Element methods for $p(x)$ -laplacian variational problems exhibiting the Lavrentiev phenomenon.

4.1 Ensuring Convergence to the Narrow Solution

Proposition 6 *In the setting of Theorem 4, regarding the discretization $p^{\mathfrak{D}^n} = (p_D)_{D \in \mathfrak{D}^n} \in \mathbb{R}^{\mathfrak{D}^n}$ of the variable exponent $p(\cdot)$ on the diamond mesh, instead of (16) assume that*

$$p_D = \operatorname{ess\,sup}_D p(\cdot). \tag{33}$$

In addition, assume that the scheme possesses the following property:

there exists a sequence $\tilde{u}^{\mathfrak{T}^n}$ of $W_0^{1,\infty}(\Omega)$ functions such that

$$\|\nabla^{\mathfrak{D}^n} \tilde{u}^{\mathfrak{T}^n} - \nabla \tilde{u}^{\mathfrak{T}^n}\|_{L^{p^{\mathfrak{D}^n}(\cdot)}} \rightarrow 0 \text{ as } n \rightarrow \infty. \tag{34}$$

Then the conclusion of Theorem 4 can be replaced by the conclusion of convergence to the narrow weak solution of the problem.

Informally speaking, one can consider (34) as a conformity assumption on the scheme, since the discrete solution can be replaced—up to a negligible error in the appropriate norm—by a continuous function on Ω .

Remark 2 We stress that the assumption (34) is trivially verified for the CVFE scheme, by taking $\tilde{u}^{\mathfrak{T}} := \sum_{K \in \mathfrak{T}} u_K \varphi_K$, where $(\varphi_K)_{K \in \mathfrak{T}}$ is the basis of \mathbb{P}_1 shape functions on the triangular mesh \mathfrak{T} (the CVFE scheme can be seen as a mass-lumped conforming Finite

Element scheme). Indeed, the CVFE construction simply means $\nabla^{\mathcal{D}_n} u^{\bar{x}_n} := \nabla \tilde{u}^{\bar{x}_n}$. On the contrary, the assumption (34) is not a natural assumption for the DDFV scheme (which is witnessed, in particular, by the possible discrepancy between $u^{\mathfrak{M}_n}$ and $u^{\mathfrak{M}_n^*}$ which led us to introduce a penalization into the scheme). More generally, the requirement (34) is related to the energy estimate (22) and its fulfillment may depend on the choice of the mesh. E.g., in the situation of piecewise constant variable exponent $p(\cdot)$ (that includes the Zhikov counterexample (4)) one could consider piecewise application of the lifting construction of [11]—developed for constant p —to produce the continuous interpolates $\tilde{u}^{\bar{x}_n}$ of $u^{\bar{x}_n}$. Here, we do not pursue the verification of (34) beyond the trivial CVFE case.

Proof The proof of Proposition 6 differs from the one of Theorem 4 mainly at the point where u should be inserted as an admissible test function in (23), in the place of a smooth test function. To ensure this is possible, we first observe that due to (33), one has $p^{\mathcal{D}} \geq p(\cdot)$ and therefore, from the energy estimate (22), $\mathcal{G} = \nabla u$ is also the limit, in the weak $(L^{p(\cdot)}(\Omega))^2$ topology, of (a subsequence of) $\nabla^{\mathcal{D}} u^{\bar{x}_n}$. Then, because of $p^{\mathcal{D}} \geq p(\cdot)$, (34) implies that ∇u is also the weak limit of (a subsequence of) $\nabla \tilde{u}^{\bar{x}_n}$, which are $W_0^{1,\infty}(\Omega)$ functions and can be approximated, in turn, by \mathbf{H} functions in the norm of \mathbf{H} . The resulting approximation, with gradients weakly convergent in $(L^{p(\cdot)}(\Omega))^2$, is enough to ensure that u can be taken as a test function in the left-hand side of (23); note that the assumption $f \in L^{(p-\cdot)'(\Omega)}$ permits to pass to the limit in the right-hand side of (23). Starting from this point, as in Theorem 4 we find that u fulfills the distributional formulation of problem (1), (2), moreover, the convergences (18), (19) hold.

To state that u is a narrow weak solution of the problem, it remains to assert that $u \in \mathbf{H}$. To this end, we upgrade the above claim of weak $(L^{p(\cdot)}(\Omega))^2$ convergence of $\nabla \tilde{u}^{\bar{x}_n}$ towards ∇u to the strong convergence. Observe that (19) implies the equi-integrability of the L^1 functions $|\nabla^{\mathcal{D}_n} u^{\bar{x}_n}|^{p^{\mathcal{D}_n}}$, and because $p^{\mathcal{D}} \geq p(\cdot)$ this also means that the functions $|\nabla^{\mathcal{D}_n} u^{\bar{x}_n}|^{p(\cdot)}$ are equi-integrable. Recalling that $\nabla u \in (L^{p(\cdot)}(\Omega))^2$, we find that $|\nabla u - \nabla^{\mathcal{D}_n} u^{\bar{x}_n}|^{p(\cdot)}$ are equi-integrable as well, moreover, due to (18) these functions converge a.e. to zero. By the Vitali theorem, we conclude that $\rho_{p(\cdot)}(\nabla u - \nabla^{\mathcal{D}_n} u^{\bar{x}_n}) \rightarrow 0$ as $n \rightarrow \infty$. By Proposition 1.2, it follows that the norm $\|\cdot\|_{L^{p(\cdot)}}$ of the difference $\nabla u - \nabla^{\mathcal{D}_n} u^{\bar{x}_n}$ vanishes as well at the limit. We conclude using the triangle inequality for $\|\cdot\|_{L^{p(\cdot)}}$. Indeed, recall that (34) and the fact that $p^{\mathcal{D}} \geq p(\cdot)$ imply that the difference $\nabla^{\mathcal{D}_n} u^{\bar{x}_n} - \nabla \tilde{u}^{\bar{x}_n}$ is vanishing, as $n \rightarrow \infty$, in the sense of the $L^{p(\cdot)}$ norm. Whence the required claim follows. \square

4.2 Prospecting Convergence to the Broad Solution

Proposition 7 *In the setting of Theorem 4, regarding the discretization $p^{\mathcal{D}_n} = (p_D)_{D \in \mathcal{D}_n} \in \mathbb{R}^{\mathcal{D}_n}$ of the variable exponent $p(\cdot)$ on the diamond mesh, instead of (16) assume that*

$$p_D = \operatorname{ess\,inf}_D p(\cdot). \tag{35}$$

In addition, assume that the discrete framework at hand possesses the strong approximation property of the space \mathbf{W} , namely, beyond (11), for all $\phi \in \mathbf{W}$ there exist $\phi^{\bar{x}_n} \in \mathbb{R}^{\bar{x}_n}$ such that

$$\|\phi^{\bar{x}_n} - \phi\|_{L^{p(\cdot)}} \rightarrow 0 \quad \text{and} \quad \|\nabla^{\mathcal{D}_n} \phi^{\bar{x}_n} - \nabla \phi\|_{L^{p(\cdot)}} \rightarrow 0 \quad \text{as } n \rightarrow \infty. \tag{36}$$

Then the conclusion of Theorem 4 can be replaced by the conclusion of convergence to the broad weak solution of the problem.

Remark 3 The above proposition is a conditional result, indeed at the present stage, we are not able to verify the assumption (36) theoretically. However, in the context of the Zhikov counterexample (4), it is known that \mathbf{H} is of codimension 1 in \mathbf{W} ; and the density of smooth functions in \mathbf{H} ensures (36) for $\phi \in \mathbf{H}$. Therefore in practice, in order to conclude that the scheme with the choice (35) approximates the broad solution, it is enough to observe that it is able to approximate \tilde{u}_0 verifying (6). The below numerical examples show that this is feasible, in particular, for the DDFV scheme which is non-conforming - contrarily to the CVFE scheme, - and thus it may indeed possess the strong approximation property for the wider space \mathbf{W} .

Proof The proof of Proposition 6 differs from the one of Theorem 4 only at the point where discrete test functions are taken into the scheme in order to derive (23). To ensure that it is possible to use discrete functions approximating any element of \mathbf{W} , we first observe that due to (33), one has $p^{\mathfrak{D}} \leq p(\cdot)$. Given a test function $\phi \in \mathbf{W}$, we use (36) to produce a sequence of discrete test functions to be inserted into the scheme (17). The $L^{p(\cdot)}$ convergences required in (36) permit to pass to the limit in the resulting identities, having in mind the energy bound (22) and the inequality $p^{\mathfrak{D}} \leq p(\cdot)$; at the limit, we infer (23). \square

4.3 Numerical Experiments on Zhikov’s Counterexample

The aim of this paragraph is to numerically capture the two different solutions, namely the \mathbf{W} -solution and the \mathbf{H} -solution, in the case where $p(\cdot)$ is discontinuous. For this purpose, we focus on the counterexample of Zhikov recalled in Section 2. We take the nonlinearity (2) with $p(\cdot)$ as given in (4), and consider u_0 defined in (5). Referring to Fig. 1, u_0 is equal to 1 (respectively to -1) on the upper (resp., on the lower) white triangle and $x_2/|x_1|$ on the hatched zone in Fig. 1.

We keep the same set up as previously when using the CVFE solver. A similar resolution process is extended to the context of the DDFV scheme on the same meshes. Figures 6 and 7 show the distribution of the discretized variable exponent $p^{\mathfrak{D}}$ around the origin, in the context of the CVFE method and the DDFV method respectively. Recall that $p(\cdot)$ is piecewise constant on the diamonds (triangles, in the CVFE context; quadrangles, in the DDFV one).

In what follows, we compare and illustrate the obtained results using both methods with two different examples.

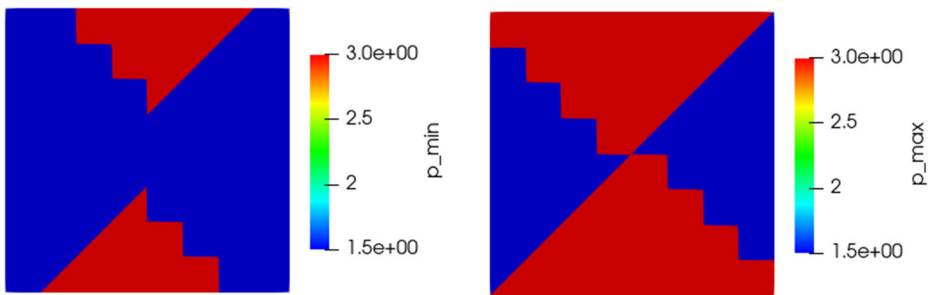


Fig. 6 Magnification on the shape of the power function $p(\cdot)$ around the origin using $p = p_{\min}$ (left) and $p = p_{\max}$ (right) in the framework of the CVFE method

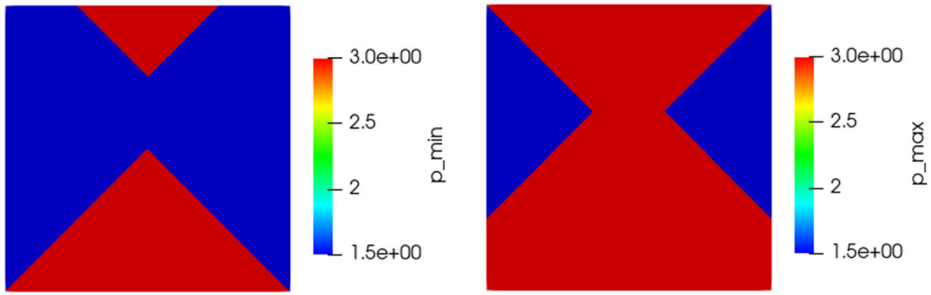


Fig. 7 Magnification on the shape of the power function $p(\cdot)$ around the origin using $p = p_{\min}$ (left) and $p = p_{\max}$ (right) in the framework of the DDFV method

4.3.1 Test 4a

Consider the $p(x)$ -Laplacian problem without forcing term but supplemented with non-homogeneous Dirichlet boundary conditions borrowed from [17]:

$$\begin{cases} -\operatorname{div} (|\nabla u|^{p(x)-2} \nabla u) = 0, \\ u|_{\partial\Omega} = \alpha u_0, \quad \text{where } \alpha > 1 \text{ is large enough.} \end{cases}$$

The parameter α is set to 10. Figure 8 plots the obtained approximate solution using two constant piecewise discretizations of p_h per triangles. For each triangle D , the first (resp. second) one consists in taking the minimum (resp. maximum) of the values of p at the vertices of D . As a consequence, both solutions are completely different. Indeed, the one corresponding to $p_{\max}(\cdot)$ is entirely continuous, including the area surrounding the origin. This can be qualified as the narrow (or the **H**-) solution. The other one corresponding to $p_{\min}(\cdot)$ is singular at 0 and resembles to u_0 . It can be then qualified as the broad (or the **W**-) solution.

In addition to the CVFE method which is conforming, we make use of the non-conforming DDFV strategy. Quite analogous outcomes are noticed, see Fig. 9. In this case, the max and min of the discrete exponent are performed on the diamond cells.

To sum up, in this test we observe that the choice (33) (resp., (35)) for discretization of $p(\cdot)$ permits to approximate the narrow (resp., the broad) solution, irrespective of the conformity of the underlying scheme.

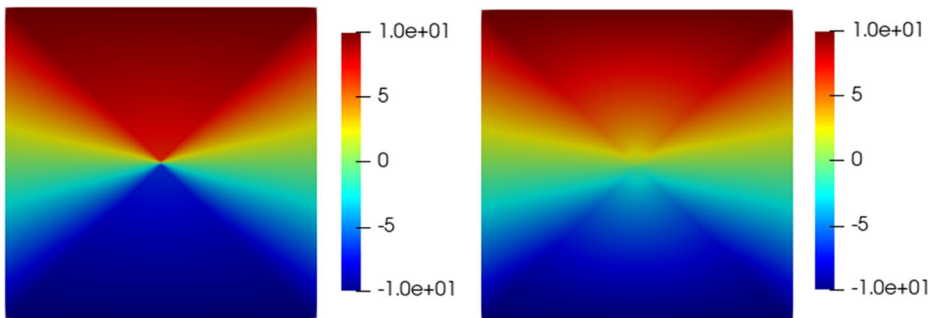


Fig. 8 Numerical solution by the CVFE method with $p_{\min}(\cdot)$ (left) and $p_{\max}(\cdot)$ (right) over each triangle

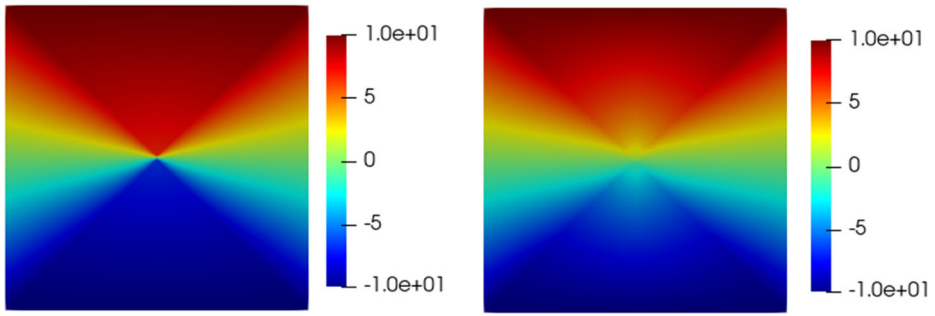


Fig. 9 Numerical solution by the DDFV method with $p_{\min}(\cdot)$ (left) and $p_{\max}(\cdot)$ (right) over each diamond

4.3.2 Test 4b

In this last test-case, we consider the setting (1), (2), (4) with a specific numerical procedure for computation of the source term. The originality of this example is to impose the function

$$u(x) = (1 - x_1^2 - x_2^2)^+ u_0(x),$$

as the broad (**W**-) solution that is evaluated at the vertices of the mesh, see Fig. 10. In other words, we compute the discrete left-hand side of (1) using the CVFE scheme, where according to the above results on approximation of broad solutions, the discretized variable exponent is defined as $p_{\min}(\cdot)$. The resulting per volume values are set to define the discrete source term in the right-hand side (RHS). Note that by this choice, the resulting scheme approximates the broad solution u by construction.

Now, keeping the same mesh, we take this discrete RHS in the CVFE algorithm with $p_{\max}(\cdot)$ discretization of the variable exponent. As Fig. 11 shows, the obtained numerical solution is different from the imposed one. It is clearly regular around $x = 0$ and therefore, we assimilate it to the narrow (**H**-) solution. This highlights the importance of the conformity assumption (34) for the approximation of the narrow solution.

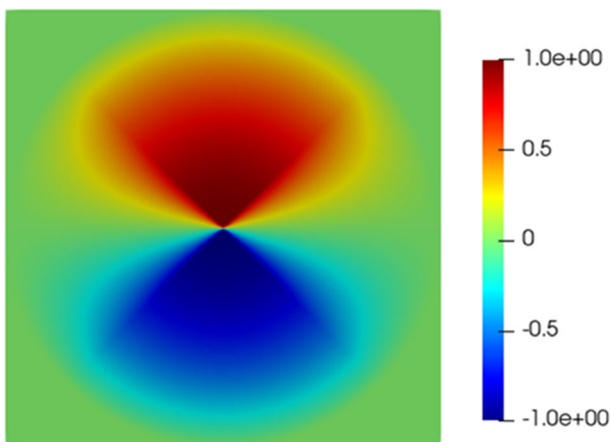


Fig. 10 Discretized continuous solution $u_e(x_K)$ with $p_{\min}(\cdot)$ over each triangle

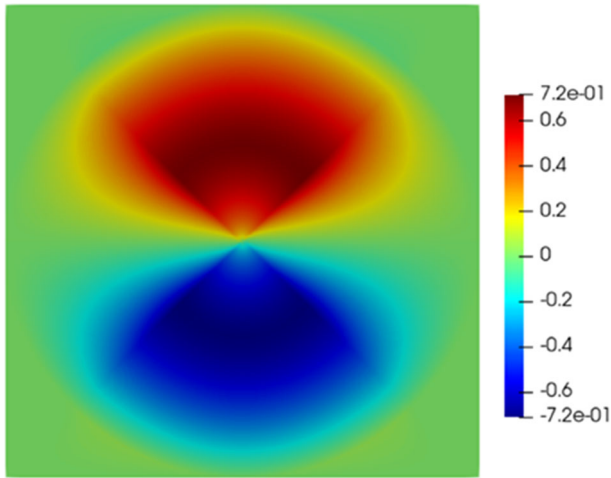


Fig. 11 Numerical solution by the CVFE method with $p_{\max}(\cdot)$ over each triangle. The right-hand side is computed using the CVFE scheme

We repeat a similar experience by computing this time the RHS using the DDFV scheme with $p_{\min}(\cdot)$ -discretization. We inject this term in the DDFV algorithms with $p_{\max}(\cdot)$ -approximation of $p(\cdot)$. In light of Fig. 12, the found solution is in great accordance with the imposed one, meaning that only the \mathbf{W} -solution is detected.

Through this example we observe that, on the one hand, the non-conforming nature of the DDFV scheme may preclude it from approximating the narrow solution; while on the other hand, the DDFV scheme seems to possess the approximation property (36) of the space \mathbf{W} , at least in the setting of the Zhikov counterexample.

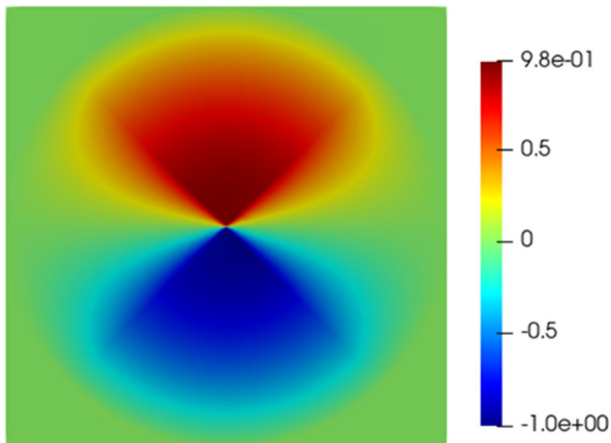


Fig. 12 Numerical solution by the DDFV method with $p_{\max}(\cdot)$ over each diamond. The right-hand side is computed using the DDFV scheme

5 Conclusions

We pointed out that the technique of [7], based upon the Young-measure description of the weak L^1 convergence, is suitable for assessing convergence of consistent numerical schemes for the $p(x)$ -laplacian kind problem, at least in the standard case with log-Hölder regular exponent; the strategy of the proof easily extends to $p(u)$ - and $p[u]$ -laplacian problems.

In the more general situation involving a Lavrentiev gap $\mathbf{W} \setminus \mathbf{H} \neq \emptyset$, we describe the specific strategies for separate approximation of the \mathbf{H} - and the \mathbf{W} - solutions, and illustrate them numerically. Our results and experiments demonstrate that the choice of $p_D = \max_D p$ (respectively of $p_D = \min_D p$) is particularly important for the selection of the \mathbf{H} -solution (resp., of the \mathbf{W} -solution) and that the conformity (resp., the non-conformity) of the underlying approximation is another important criterion for successful approximation of these dissimilar solutions. These conclusions corroborate, in the Finite Volume setting, the conclusions of the recent work [17] for the Finite Element setting.

Acknowledgements We thank the reviewers of this paper for a careful reading and for many useful remarks. This paper has been supported by the RUDN University Strategic Academic Leadership Program.

References

1. Afif, M., Amaziane, B.: Convergence of finite volume schemes for a degenerate convection–diffusion equation arising in flow in porous media. *Comput. Methods Appl. Mech. Eng.* **191**, 5265–5286 (2002)
2. Alkhutov, Yu.A.: Elliptic problems with nonstandard conditions of growth: Zhikov’s approach. *Complex Var. Elliptic Equ.* **56**, 559–571 (2011)
3. Alnashri, Y., Droniou, J.: A gradient discretization method to analyze numerical schemes for nonlinear variational inequalities, application to the seepage problem. *SIAM. J. Numer. Anal.* **56**, 2375–2405 (2018)
4. Andreianov, B., Bendahmane, M., Hubert, F.: On 3D DDFV discretization of gradient and divergence operators: discrete functional analysis tools and applications to degenerate parabolic problems. *Comput. Methods Appl. Math.* **13**, 369–410 (2013)
5. Andreianov, B., Bendahmane, M., Karlsen, K.H.: A gradient reconstruction formula for finite volume schemes and discrete duality. In: Eymard, R., Hérard, J.-M. (eds.), *Finite Volumes For Complex Applications V*, pp 161–168. ISTE, London (2008)
6. Andreianov, B., Bendahmane, M., Karlsen, K.H.: Discrete duality finite volume schemes for doubly nonlinear degenerate hyperbolic-parabolic equations. *J. Hyperbolic Differ. Equ.* **7**, 1–67 (2010)
7. Andreianov, B., Bendahmane, M., Ouaro, S.: Structural stability for variable exponent elliptic problems, I. The $p(x)$ -Laplacian kind problems. *Nonlinear Anal.* **73**, 2–24 (2010)
8. Andreianov, B., Bendahmane, M., Ouaro, S.: Structural stability for variable exponent elliptic problems, II. The $p(u)$ -Laplacian and coupled problems. *Nonlinear Anal.* **72**, 4649–4660 (2010)
9. Andreianov, B., Boyer, F., Hubert, F.: Finite volume schemes for the p -Laplacian on Cartesian meshes. *ESAIM Math. Model. Numer. Anal.* **38**, 931–959 (2004)
10. Andreianov, B., Boyer, F., Hubert, F.: Discrete duality finite volume schemes for Leray–Lions-type elliptic problems on general 2D meshes. *Numer. Methods Partial Differ. Equ.* **23**, 145–195 (2007)
11. Andreianov, B., Gutnic, M., Wittbold, P.: Convergence of finite volume approximations for a nonlinear elliptic-parabolic problem : a “continuou” approach. *SIAM J. Numer. Anal.* **42**, 228–251 (2004)
12. Andreianov, B., Quenjel, E.H.: Nodal discrete duality numerical scheme for nonlinear diffusion problems on general meshes. Preprint <https://hal.archives-ouvertes.fr/hal-03739675> (2022)
13. Antonietti, P., Beirão da Veiga, L., Bigoni, N., Verani, M.: Mimetic finite differences for nonlinear and control problems. *Math. Models. Methods Appl. Sci.* **24**, 1457–1493 (2014)
14. Antontsev, S.N., Rodrigues, J.F.: On stationary thermo-rheological viscous flows. *Ann. Univ. Ferrara Sez. VII Sci. Mat.* **52**, 19–36 (2006)

15. Antontsev, S.N., Shmarev, S.I.: Elliptic equations with anisotropic nonlinearity and nonstandard growth conditions. In: Chipot, M., Quittner, P. (Eds.) *Handbook of Differential Equations: Stationary Partial Differential Equations*, pp. 1–100. Elsevier (2005)
16. Balci, A.Kh., Diening, L., Surnachev, M.: New examples on Lavrentiev gap using fractals. *Calc. Var. Partial Differ. Equ.* **59**, 180 (2020)
17. Balci, A.Kh., Ortner, C., Storn, J.: Crouzeix–Raviart finite element method for non-autonomous variational problems with Lavrentiev gap. *Numerische Mathematik* **151**, 1–27 (2022)
18. Ball, J.M.: A version of the fundamental theorem for young measures. In: Rascle, M., Serre, D., Slemrod, M. (eds.) *PDEs and Continuum Models of Phase Transitions* (Nice, 1988). *Lecture Notes in Physics*, vol. 344, pp. 207–215. Springer, Berlin, Heidelberg (1989)
19. Barrett, J.W., Liu, W.B.: A remark on the regularity of the solutions of the p -Laplacian and its application to their finite element approximation. *J. Math. Anal. Appl.* **178**, 470–487 (1993)
20. Barrett, J.W., Liu, W.B.: Finite element approximation of the p -Laplacian. *Math. Comput.* **61**, 523–537 (1993)
21. Bendahmane, M., Wittbold, P.: Renormalized solutions for nonlinear elliptic equations with variable exponents and L^1 data. *Nonlinear Anal.* **70**, 567–583 (2009)
22. Bendahmane, M., Wittbold, P., Zimmermann, A.: Renormalized solutions for a nonlinear parabolic equation with variable exponents and L^1 -data. *J. Differ. Equ.* **249**, 1483–1515 (2010)
23. Bessemoulin-Chatard, M., Chainais-Hillairet, C., Filbet, F.: On discrete functional inequalities for some finite volume schemes. *IMA J. Numer. Anal.* **35**, 1125–1149 (2015)
24. Breit, D., Diening, L., Schwarzacher, S.: Finite element approximation of the $p(\cdot)$ -Laplacian. *SIAM J. Numer. Anal.* **53**, 551–572 (2015)
25. Browder, F.E.: Existence theorems for nonlinear partial differential equations. In: Chern, S.-S., Smale, S. (eds.) *Global Analysis* (Berkeley, California, 1968). *Proceedings of Symposia in Pure Mathematics*, vol. 16, pp. 1–60. American Mathematical Society, Providence, RI (1970)
26. Cai, Z.Q.: On the finite volume element method. *Numer. Math.* **58**, 713–735 (1990)
27. Chen, Y., Levine, S., Rao, M.: Variable exponent, linear growth functionals in image restoration. *SIAM J. Appl. Math.* **66**, 1383–1406 (2006)
28. Chow, S.-S.: Finite element error estimates for non-linear elliptic equations of monotone type. *Numer. Math.* **54**, 373–393 (1989)
29. Coudière, Y., Hubert, F.: A 3D discrete duality finite volume method for nonlinear elliptic equations. *SIAM J. Sci. Comput.* **33**, 1739–1764 (2011)
30. Diening, L., Harjulehto, P., Hästö, P., Růžička, M.: *Lebesgue and Sobolev Spaces with Variable Exponents*. *Lecture Notes in Mathematics*, vol. 2017. Springer, Heidelberg (2011)
31. Diening, L., Nägele, P., Růžička, M.: Monotone operator theory for unsteady problems in variable exponent spaces. *Complex Var. Elliptic Equ.* **57**, 1209–1231 (2012)
32. Di Pietro, D.A., Droniou, J.: A hybrid high-order method for Leray–Lions elliptic equations on general meshes. *Math. Comput.* **86**, 2159–2191 (2017)
33. Dolzmann, G., Hungerbühler, N., Müller, S.: Non-linear elliptic systems with measure-valued right-hand side. *Math. Z.* **226**, 545–574 (1997)
34. Domelevo, K., Omnes, P.: A finite volume method for the Laplace equation on almost arbitrary two-dimensional grids. *ESAIM Math. Model. Numer. Anal.* **39**, 1203–1249 (2005)
35. Droniou, J.: Finite volume schemes for fully non-linear elliptic equations in divergence form. *ESAIM Math. Model. Numer. Anal.* **40**, 1069–1100 (2006)
36. Droniou, J.: Finite volume schemes for diffusion equations: Introduction to and review of modern methods. *Math. Models Methods Appl. Sci.* **24**, 1575–1619 (2014)
37. Droniou, J., Eymard, R., Gallouët, T., Guichard, C., Herbin, R.: *The Gradient Discretisation Method*. *Mathématiques et Applications*, vol. 82. Springer, Cham (2018)
38. Eymard, R., Gallouët, Th., Herbin, R.: Finite volume methods. In: Ciarlet, P.G., Lions, J.L. (eds.), *Handbook of Numerical Analysis*, vol. VII, pp. 713–1020. North-Holland (2000)
39. Fan, X.: Regularity of nonstandard Lagrangians $f(x, \xi)$. *Nonlinear Anal.* **27**, 669–678 (1996)
40. Fan, X., Zhao, D.: On the spaces $L^{p(x)}(\Omega)$ and $W^{m,p(x)}(\Omega)$. *J. Math. Anal. Appl.* **263**, 424–446 (2001)
41. Fuhrmann, J., Glitzy, A., Liero, M.: Hybrid finite-volume/finite-element schemes for $p(x)$ -Laplace thermistor models. In: Cancès, C., Omnes, P. (eds.) *Finite Volumes for Complex Applications VIII - Hyperbolic, Elliptic and Parabolic Problems*. *Springer Proceedings in Mathematics & Statistics*, vol. 200, pp. 397–405. Springer, Cham (2017)
42. Ghilani, M., Quenjel, E.H., Rhoudaf, M.: Numerical analysis of a stable finite volume scheme for a generalized thermistor model. *Comput. Methods Appl. Math.* **21**, 69–87 (2021)
43. Guibé, O., Leclavier, S.: Finite volume scheme and renormalized solutions for a noncoercive and nonlinear parabolic problem with L^1 data. Preprint hal-02424104 (2019)

44. Hungerbühler, N.: A refinement of Ball's theorem on Young measures. *New York J. Math.* **3**, 48–53 (1997)
45. Hungerbühler, N.: Quasi-linear parabolic systems in divergence form with weak monotonicity. *Duke Math. J.* **107**, 497–520 (2001)
46. Leclavier, S.: Finite volume scheme and renormalized solutions for a noncoercive elliptic problem with l^1 data. *Comput. Methods Appl. Math.* **17**, 85–104 (2017)
47. Lions, J.L.: *Quelques Méthodes de résolution des Problèmes aux limites non linéaires*. Dunod, Paris (1969)
48. Minty, G.J.: Monotone (nonlinear) operators in Hilbert space. *Duke Math. J.* **29**, 341–346 (1962)
49. Pedregal, P.: *Parametrized Measures and Variational Principles*. Progress in Nonlinear Differential Equations and Their Applications, vol. 30. Birkhäuser, Basel (1997)
50. Quarteroni, A.: *Numerical models for differential problems (Translated from Italian)*, 2nd edn. MS&A, vol. 8. Springer, Milan (2014)
51. Rajagopal, K.R., Růžička, M.: *Mathematical modelling of electrorheological materials*. *Contin. Mech. Thermodyn.* **13**, 59–78 (2001)
52. Růžička, M.: *Electrorheological Fluids: Modeling and Mathematical Theory*. Lecture Notes in Mathematics, vol. 1748. Springer-Verlag, Berlin (2000)
53. Zhikov, V.V.: Averaging of functionals of the calculus of variations and elasticity theory (Russian). *Izv. Akad. Nauk SSSR Ser. Mat.* **50**, 675–710 (1986). Engl. transl. in *Mah. Ussr Izvestiya*, 29, 33–66 (1987)
54. Zhikov, V.V.: On the Lavrentiev effect (Russian). *Dokl. Akad. Nauk* **345**, 10–14 (1995)
55. Zhikov, V.V.: Density of smooth functions in Orlicz-Sobolev spaces (Russian), vol. 310. Engl. transl. in *J. Math. Sci.*, 132, 285–294 (2006) (2004)
56. Zhikov, V.V.: Solvability of the three-dimensional thermistor problem (Russian). *Trudy Mat. Inst. Steklov* **261**, 101–114 (2008). Engl. transl. in *Proc. Steklov Inst. Math.*, 261, 1–14, (2008)
57. Zhikov, V.V.: On passage to the limit in nonlinear elliptic equations. *Dokl. Math.* **77**, 383–387 (2008)
58. Zhikov, V.V.: On the technique for passing to the limit in nonlinear elliptic equations. *Funct. Anal. Appl.* **43**, 96–112 (2009)
59. Zhikov, V.V.: On variational problems and nonlinear elliptic equations with nonstandard growth conditions. *J. Math. Sci. (N.Y.)* **173**, 463–570 (2011)

Publisher's Note Springer Nature remains neutral with regard to jurisdictional claims in published maps and institutional affiliations.

Springer Nature or its licensor holds exclusive rights to this article under a publishing agreement with the author(s) or other rightsholder(s); author self-archiving of the accepted manuscript version of this article is solely governed by the terms of such publishing agreement and applicable law.